



Short-term middle Eocene (Bartonian) paleoenvironmental changes in the sedimentary succession of Olivetta San Michele (NW Italy): the response of shallow-water biota to climate in NW Tethys

Luca Arena¹ · Victor M. Giraldo-Gómez¹ · Andrea Baucon¹ · Michele Piazza¹ · Cesare A. Papazzoni² · Johannes Pignatti³ · Antonella Gandolfi¹ · Antonino Briguglio¹

Received: 1 June 2023 / Accepted: 14 November 2023
© The Author(s) 2024

Abstract

This study focuses on the paleontological content of the middle Eocene (Bartonian) carbonate–siliciclastic sediments of the Capo Mortola Calcarene Formation from Olivetta San Michele (Liguria, Italy). Along the succession, there are significant paleoecological changes triggered by the variation in neritic input as a consequence of tectonic and climatic instability. Among microfossils, nummulitids prevail, followed by orthophragmines, smaller benthic, and planktonic foraminifera, whereas mollusks and ichnofossils are the most abundant macrofossils. The sudden changes in the benthic communities due to the progressive increase in fluvial input are recorded throughout the sedimentary succession. An increase in water turbidity caused stressful conditions for autotrophic taxa, reducing their size and abundance. In contrast, filter feeders became dominant, suggesting an increase in dissolved and suspended nutrients. Ichnological analysis shows environmental fluctuations controlled by the transport of neritic material offshore, thus confirming the general deepening trend of the studied succession. In the upper part of the succession, we recorded an alternation between gravity flows and marly sediments that are interpreted as short-term alternations between low and intense precipitations. The gravity flows yield taxa such as larger benthic foraminifera (LBF), smaller benthic and planktonic foraminifera, mollusks, and corals. In turn, marls display only a few LBF and abundant smaller benthic and planktonic foraminifera. In these intervals, the increase in planktonic foraminifera also suggests a deepening of the carbonate ramp coinciding with a reduction of light that did not favor the development of LBF. These changes are probably related to the climatic dynamics that occurred in the Bartonian in the western Tethys.

Keywords Paleoecology · Macrofauna · Larger benthic foraminifera · Ichnofossils · Photic zone · Carbonate ramp

Introduction

The Eocene is considered a critical epoch in terms of variation in both paleogeographic setting and climatic dynamics (e.g., Zachos et al. 2001; Torsvik and Cocks 2016). A

global greenhouse climate, characterized by high temperatures in the early Eocene (Early Eocene Climatic Optimum: EECO; Zachos et al. 2001, 2008; Bijl et al. 2009; Hollis et al. 2010, 2012), was followed by a long-term cooling that was interrupted by a global warming event during the late middle Eocene (Middle Eocene Climatic Optimum: MECO; Zachos et al. 2001; Bohaty and Zachos 2003; Bohaty et al. 2009; Sluijs et al. 2013). The interplay between global and regional climate processes and the biosphere response have been largely documented for the Eocene deep-water settings (e.g., Ivany et al. 2008; Deprez et al. 2015; Boscolo Galazzo et al. 2016; Giraldo-Gómez et al. 2017; Luciani et al. 2017; Foster et al. 2020; Marchegiano and John 2022).

In contrast, shallow-water depositional settings such as carbonate platforms or mixed carbonate–siliciclastic systems, as recorded in the Mediterranean region (NW Tethys), are much less studied with respect to global climatic and

✉ Victor M. Giraldo-Gómez
victormanuel.giraldogomez@edu.unige.it

¹ Dipartimento di Scienze della Terra, dell'Ambiente e della Vita, Università degli Studi di Genova, Corso Europa 26, 16132 Genoa, Italy

² Dipartimento di Scienze Chimiche e Geologiche, Università di Modena e Reggio Emilia, Via Campi 103, 41125 Modena, Italy

³ Dipartimento di Scienze della Terra, Università degli Studi di Roma "La Sapienza", Piazzale Aldo Moro 5, 00185 Rome, Italy

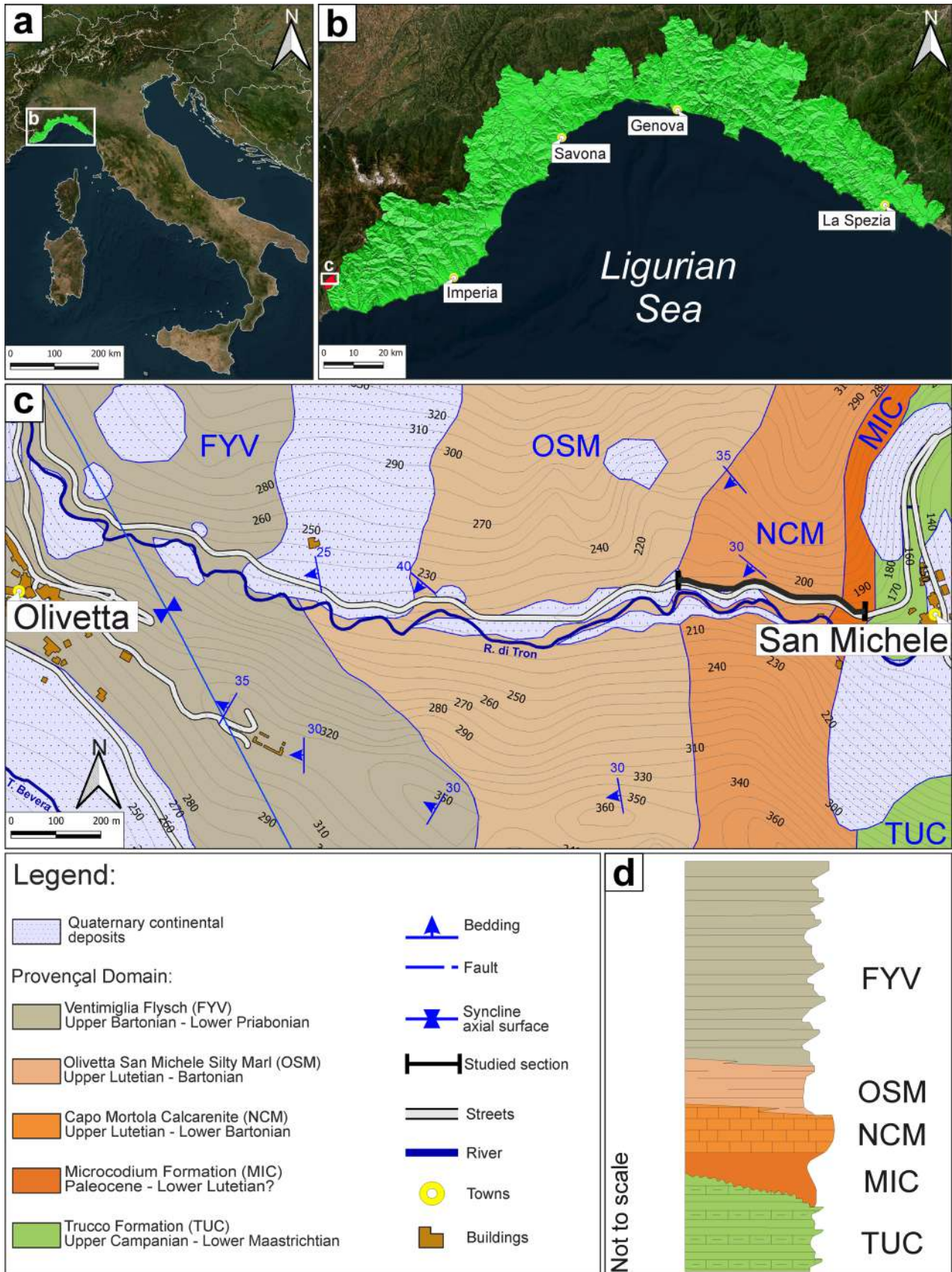


Fig. 1 **a** Map of Italy showing the Liguria region highlighted in green (modified from https://server.arcgisonline.com/ArcGIS/rest/services/World_Imagery). **b** Location map of the Liguria region displaying the municipality of the Olivetta San Michele (modified from https://server.arcgisonline.com/ArcGIS/rest/services/World_Imagery). **c** Detailed geological map of Olivetta San Michele area, showing the studied section, modified from Dallagiovanna et al. (2012b). **d** Simplified stratigraphic column of the study area modified from Decarlis et al. (2014)

environmental perturbations. These sedimentary successions yield an extraordinary diversity of both micro- and macrofauna that during the Eocene experienced the effects of climate change, as evidenced by high water temperatures, increased continental weathering, and shifting hydrological cycles (e.g., Martín-Martín et al. 2021; Coletti et al. 2021; Brandano and Tomassetti 2022; Bosellini et al. 2022; Briguglio et al. 2024).

The paleogeographic setting of the Ligurian Alps (Italy) and the Provençal Domain (Gèze and Nestéroff 1968; Lanteaume 1968; Lemoine et al. 1986; Ford et al. 2006; de Graciansky et al. 2010; Giammarino et al. 2010; Dallagiovanna et al. 2012a; Seno et al. 2012; Decarlis et al. 2014) provides extended sedimentary successions where it is possible to observe and study the resilience of micro- and macrofauna to Middle Eocene climatic perturbations.

This study aims to describe the paleoenvironmental development of the Bartonian deposits in the Olivetta San Michele section, with special emphasis on (1) the analysis of paleoecological parameters such as diversity and dominance, (2) the climatic influence exerted on specific taxa, and (3) the data retrieved from both the biota observed at outcrop scale and the one recorded in thin sections. With these aims, our goal is to describe in detail the sedimentary and ecological development of the early stages of the drowning of a middle Eocene ramp. The early stages of ramp drowning may vary rapidly along a sedimentary succession as the result of shifting ecological gradients; ecological niches for specific organisms may have a relatively short occurrence along the profile yet provide valuable insights on the evolutionary stages of the drowning. The integration of observations on macro-, microfacies, and trace fossils allowed us to reconstruct the paleoenvironmental succession.

Geological setting and studied section

The studied section is in the westernmost part of Liguria (Italy), which is part of the Provençal Domain (43°52.78140'–7°31.97550'; Fig. 1a, b). The Olivetta San Michele (Olivetta SM) section crops out along the eastern limb of the syncline of Piène–Olivetta SM (between the villages of San Michele and Olivetta, Imperia province, W Liguria; Fig. 1c) and represents a good exposure

of the Meso–Cenozoic cover of the southern Dauphinois–Provençal Domain (European plate) involved in the Pyrenean–Provençal and Alpine orogenic events (Cretaceous–Oligocene), in the deformations related to the anticlockwise rotation of the Corsica–Sardinia Block (Miocene) and, finally, in the Pliocene to Recent extensional faulting (Gèze and Nestéroff 1968; Gèze et al. 1968; Lanteaume 1968; Lemoine et al. 1986; Ford et al. 2006; de Graciansky et al. 2010; Giammarino et al. 2010; Dallagiovanna et al. 2012a, b; Seno et al. 2012; Decarlis et al. 2014; Morelli et al. 2022).

Across the latest Cretaceous to early Paleogene, the Pyrenean–Provençal orogeny uplifted the southern Provençal Domain, which emerged and was exposed to a strong erosional event that produced a widespread unconformity at the top of the Upper Cretaceous deposits (Lanteaume 1968; Apps et al. 2004; de Graciansky et al. 2010; Giammarino et al. 2010; Dallagiovanna et al. 2012a, b; Seno et al. 2012; Marini et al. 2022; Briguglio et al. 2024). During the Eocene, the thrusting of the Ligurian Alps orogenic wedge onto this part of the European plate caused this domain to evolve into a foredeep basin, with a basin-fill succession unconformably deposited upon Upper Cretaceous deposits and characterized by shallow-water limestones grading to deep-water marls covered by siliciclastic turbidite sediment. This stratigraphic succession is known as Boussac's trilogy or Sinclair's trilogy (Boussac 1912; Lanteaume 1968; Campredon 1977; Sinclair 1997; Varrone 2004; Giammarino et al. 2009, 2010; de Graciansky et al. 2010; Dallagiovanna et al. 2012a, b; Perotti et al. 2012; Seno et al. 2012; Maino and Seno 2016; Mueller et al. 2020; Marini et al. 2022, 2022).

In the study area (Fig. 1c, d), the stratigraphic section is composed of (a) marls and marly limestones (Trucco Formation; Campanian–lower Maastrichtian); (b) *Microcodium*-rich, burrowed marls with grayish to reddish patches and minor conglomerates (Microcodium Formation; generally referred to the upper Lutetian or lower Bartonian); (c) fine to coarse grained siliciclastic, mixed, and carbonate deposits of shallow-marine environment (Capo Mortola Calcarenite; upper Lutetian–lower Bartonian); (d) hemipelagic silty marls and marls (Olivetta San Michele Silty Marl; Bartonian–lower Priabonian); (e) siliciclastic turbidite deposits (Ventimiglia Flysch, upper Bartonian–lower Priabonian) (Lanteaume 1968; Sturani 1969; Campredon 1977; Pasquini et al. 2001; Varrone 2004; Varrone and Clari 2003; Giammarino et al. 2009, 2010; Dallagiovanna et al. 2012a, b; Seno et al. 2012; Perotti et al. 2012; Maino and Seno 2016; Brandano 2019; Mueller et al. 2020; Coletti et al. 2021; Marini et al. 2022; Briguglio et al. 2024).

The Olivetta SM section here presented, due to the continuous presence and abundance of *Nummulites perforatus* and *N. puschi*, is assigned to the shallow benthic zone (SBZ) 17 (lower Bartonian) according to the biostratigraphic

scheme by Serra-Kiel et al. (1998), with updates by Papazoni et al. (2017).

Material and methods

In this study, a total of 188 m of sedimentary succession was studied (Fig. 2a, b); it is part of a 230-m-long profile that starts from the *Microcodium* Formation and covers the entire Capo Mortola Calcarene Formation. The succession here presented starts after the 13.7-m-thick vegetation cover hiding the contact between the two formations.

Macrofacies analysis was made with observation directly in the field (Fig. 3) at one-meter intervals: each observation point includes abundance data (0: absent; 1: common; 2: abundant) for all visible macrofossils and the lithology by using the classification scheme by Grabau (1904) and Flügel (2012). For this classification, only the size of the components of carbonate rocks (regardless of their origin) is considered for limestones, defining three classes: calcisiltite, calcarenite, and calcirudite. If fossil content is present, they are named biocalcisiltite, biocalcarene, and biocalcirudite. Throughout the entire section, five main types of macrofossils were observed: larger benthic foraminifera (almost exclusively nummulitids), gastropods, oysters, other bivalves, and corals (Figs. 2a, b, 3; see Supplementary Table S1 for the entire dataset).

For microfacies investigation, a total of 57 rock samples (from OL-15 to OL-77) were collected (Fig. 2a, b). Two rock thin sections per sample were prepared and analyzed using a custom-made Optech GZ808 optical stereomicroscope; photos were taken with a Delta Pix by Invenio (model 6EIII) digital camera. Textures were classified following Dunham (1962), and biogenic components were identified at the most accurate taxonomic level possible (genera).

The following parameters have been estimated on all thin sections (Supplementary Table S1) and parametrized to finite numbers: (1) matrix percentage (following Folk 1959) (0: 0%; 1: 1–10%; 2: 11–50%; 3: > 50%); (2) grains roundness and grain sorting (0: poor; 1: well; 2: very well); (3) grain size (0: fine; 1: medium; 2: coarse); (4) presence of quartz, glauconite, and organic matter (0: absent; 1: common; 2: abundant); (5) taxonomic diversity including nummulitids (separating *Nummulites* and *Assilina*), orthoherminifera, smaller benthic foraminifera, planktonic foraminifera, mollusks, corals, echinoderms, and worm tubes (0: absent; 1: common; 2: abundant); and (6) special features such as diagenesis, bioturbation, deformation, and transport evidence (0: absent; 1: common; 2: abundant).

This dataset was used to build a cluster analysis using Ward's algorithm (Ward 1963) to statistically discriminate the different macro- and microfacies. Pearson's correlation coefficient, calculated for both macrofacies (0.7014) and

microfacies (0.7305), indicates significant clustering within the studied data. Clusters were then used to differentiate the evolution of the sedimentary environment along the stratigraphic sections (Fig. 4). All statistical data treatment was processed by PAST software v.4.1 (Hammer et al. 2001).

Following the multidisciplinary workflow of Crippa et al. (2018), we integrated sedimentology and body fossil paleontology with ichnological analysis. For the vertical exposures of the Olivetta SM section, the application of the ichnofabric approach was used, placing particular emphasis on those textural aspects that arise from biological reworking, i.e., ichnofabrics (Ekdale and Bromley 1983; Taylor et al. 2003). The ichnofabric analysis method is comparable to facies analysis (McIlroy 2008). Each of the stratigraphic intervals studied for ichnofabrics (sample) was approximately 50 cm to 100 cm thick. Each sample was attributed to an ichnofabric class based on (1) degree of bioturbation, quantified as percent of bioturbated area (Knaust 2021); (2) components of the ichnofabric, including either distinct trace fossils or biodeformational structures with indistinct outlines (Taylor et al. 2003; Wetzel and Uchman 1998); (3) diversity, i.e., the number of ichnotaxa present; and (4) distribution of bioturbation at the sample scale (Supplementary Table S1). Following standard ichnological practice (Bromley 1996; Taylor et al. 2003; Gingras et al. 2011, 2015; Knaust 2017), relative abundance, burrow size, tiering, trace fossil frequency, and primary sedimentology have also been observed.

Results

Macrofacies analysis (outcrop observation)

The Capo Mortola Calcarene Formation is mainly characterized by two lithotypes: limestone (calcisiltite–biocalcisiltite, calcarenite–biocalcarene, and calcirudite–biocalcirudite) and marl, as observed in the outcrop (Fig. 2a, b; Table 1 and Supplementary Table S1). Throughout the first half of the succession (42–195.75 m), a general gradation in grain size from calcisiltite to calcirudite is recorded. The upper part (195.75–215.5 m) is made of a marly succession with intercalated calcisiltite and calcarenite beds.

The macrofacies cluster analysis separates two major clusters: macrofacies A (MA) and macrofacies B (MB) (Figs. 2a, b, 4a; Table 1 and Supplementary Table S1).

Macrofacies A is characterized by intervals without visible nummulitids, and it is subdivided into three subfacies: (1) MA1 represents intervals where fossils are not recorded (barren); (2) MA2 is marked by a slight increase in abundance of corals, gastropods, and bivalves; (3) MA3 is characterized by higher diversity where gastropods, corals, bivalves, and oysters are common.

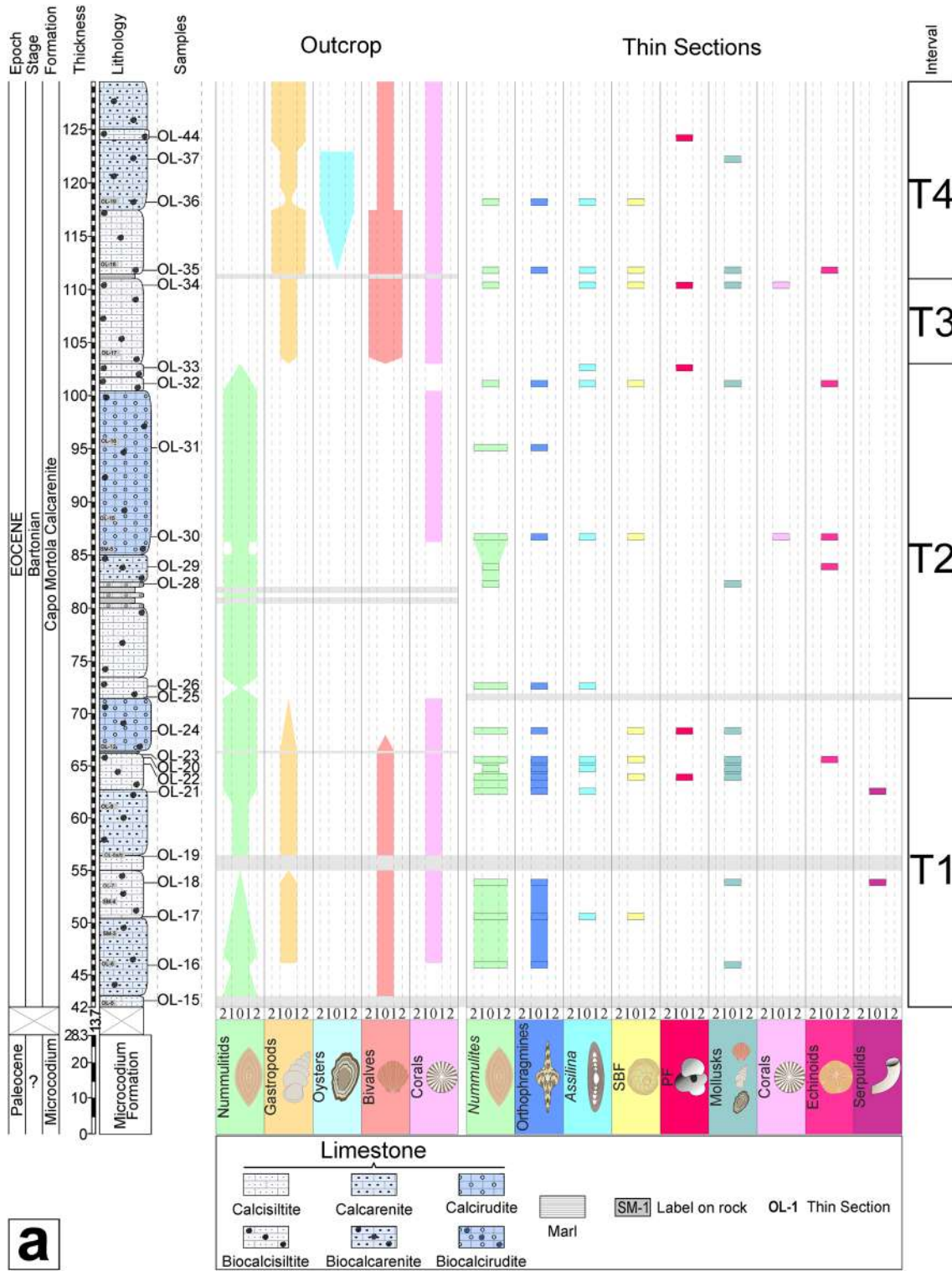
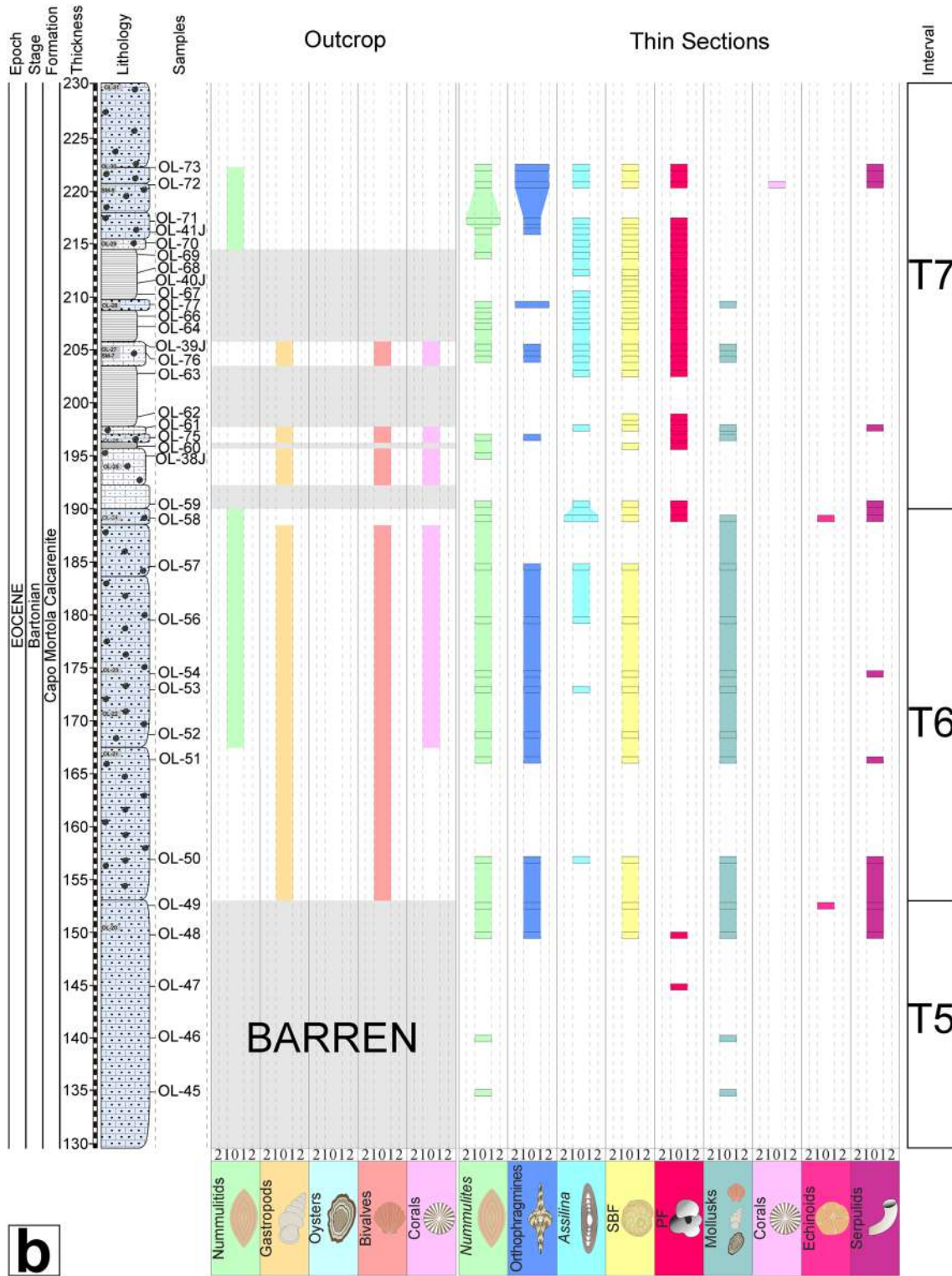


Fig. 2 Lithology and relative abundances of macro- and microfauna recorded in outcrop and thin sections of the Olivetta San Michele section (0: absent; 1: common; 2: abundant). **a** Interval of the Olivetta

San Michele section from 42 to 129.5 m. **b** Interval of the Olivetta San Michele section from 129.5 to 230 m



b

Fig. 2 (continued)

Macrofacies B is characterized by the presence of visible nummulitids and is subdivided into three subfacies: (1) MB1 is marked by the solely low abundance of nummulitids; (2) MB2 is dominated by nummulitids

and scarce corals and bivalves; (3) MB3 is characterized by the highest diversity: nummulitids are the dominant group, and gastropods, corals, and bivalves are common.

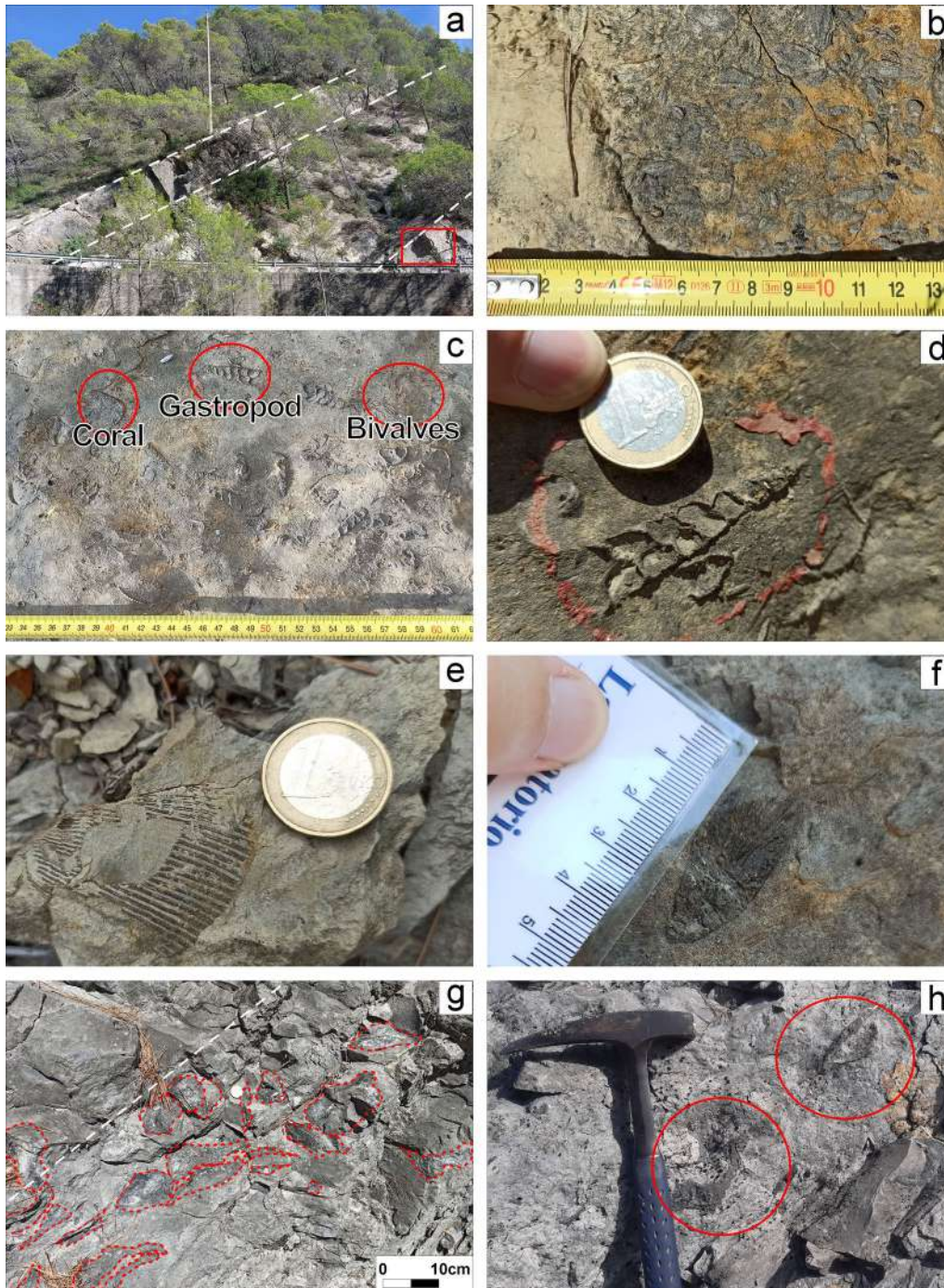


Fig. 3 Photos of the macrofauna recorded in the Olivetta San Michele section. **a** Panoramic view of the stratification layers of the Capo Mortola Calcarenite Formation in the Olivetta San Michele outcrop (around at 120th meter). **b** Layer showing abundant *Nummulites*. **c** Assemblage of bivalves, gastropods, and corals. **d** Detailed photo of

a turritellid gastropod. **e** Valve of a cardiid. **f** Fragment of a solitary scleractinian coral. **g** Oyster bed (red dashes showing different sizes of oysters). The red rectangle in **a** indicates the stratification of the layer where oysters lie. **h** Detail photo showing two valves of an oyster in life position

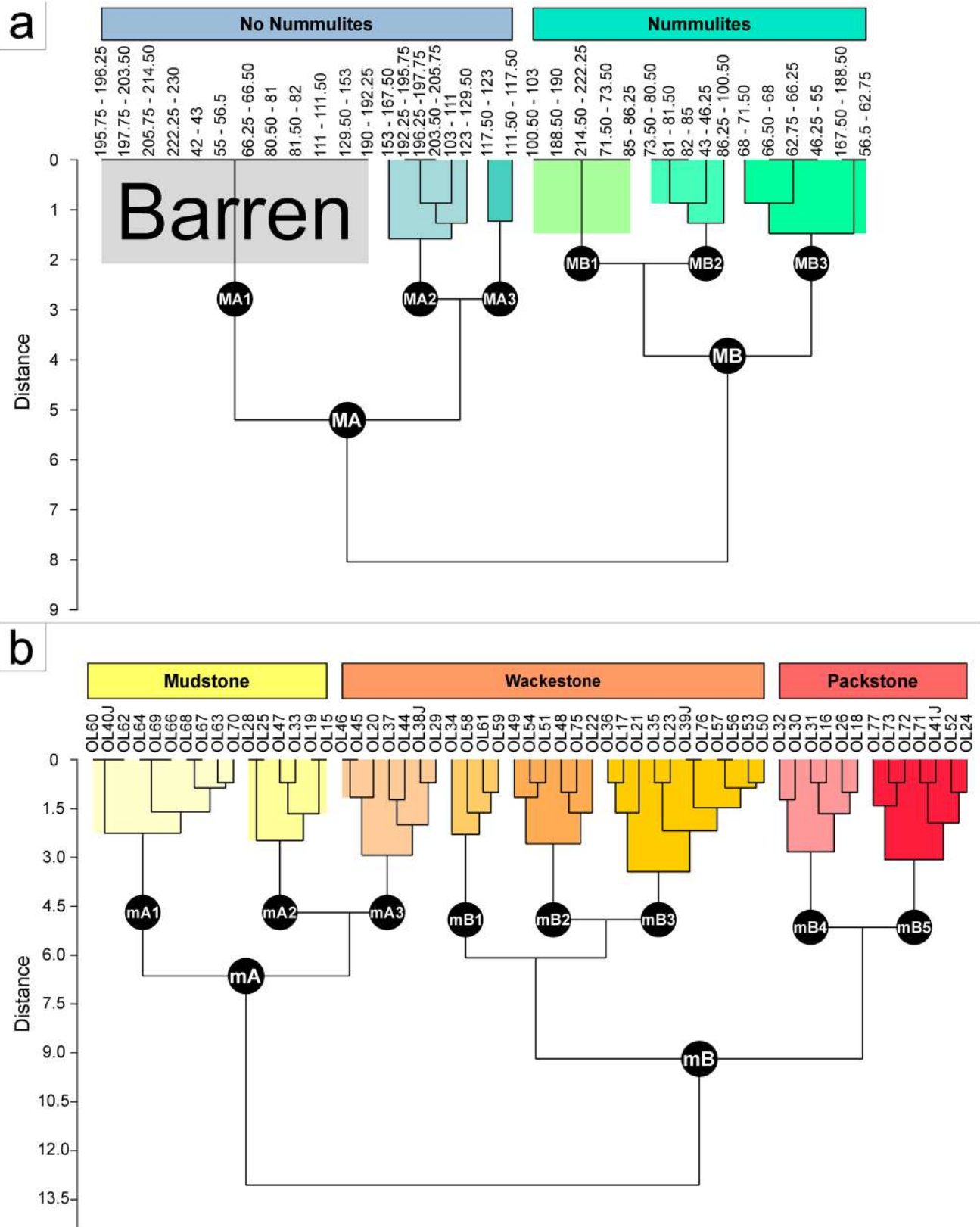


Fig. 4 Cluster analyses of the Olivetta San Michele section (Ward’s method). **a** Macrofauna (outcrop observations) cluster with indication of horizons’ thickness. **b** Microfauna (thin sections analysis) cluster with sample numbers

Table 1 Lithological description of the Olivetta San Michele section with the fossil content recorded in outcrop and thin sections

Olivetta section					
Interval	Total Thickness (m)	Layer Thickness (m)	Lithology	Fossil content	
				Outcrop	Thin Section
T7	40.00	7.25	Biocalcarenite	Not recorded	<i>Nummulites</i> , many orthofragmines, <i>Assilina</i> , SBF, PF, worms tubes
		2.00	Biocalcarenite	Nummulitids	N.a
		2.75	Biocalcarenite	Nummulitids	<i>Nummulites</i> , many orthofragmines, <i>Assilina</i> , SBF, PF, corals, worms tubes
		2.50	Biocalcarenite	Nummulitids	Many <i>Nummulites</i> , orthofragmines, <i>Assilina</i> , SBF, PF
		1.00	Biocalcilitite	Nummulitids	<i>Assilina</i> , SBF, PF
		4.75	Marl	Not recorded	<i>Nummulites</i> , <i>Assilina</i> , SBF, PF
		1.00	Calcarenite	Not recorded	<i>Nummulites</i> , many orthofragmines, <i>Assilina</i> , SBF, PF, mollusks
		3.00	Marl	Not recorded	<i>Nummulites</i> , orthofragmines, <i>Assilina</i> , SBF, PF, mollusks
		2.25	Biocalcilitite	Gastropods, bivalves, corals	<i>Nummulites</i> , orthofragmines, <i>Assilina</i> , SBF, PF, mollusks
		5.75	Marl	Not recorded	<i>Assilina</i> , SBF, PF
		0.75	Biocalcilitite	Gastropods, bivalves, corals	<i>Assilina</i> , SBF, PF, mollusks, worms tubes
		0.75	Biocalcarenite	Gastropods, bivalves, corals	<i>Nummulites</i> , orthofragmines, PF, mollusks
		0.50	Marl	Not recorded	N.a
		3.50	Biocalcilitite	Gastropods, bivalves, corals	<i>Nummulites</i> , SBF, PF
		2.25	Calcilitite	Not recorded	<i>Nummulites</i> , <i>Assilina</i> , SBF, PF, worms tubes
T6	37.00	1.50	Biocalcarenite	Nummulitids	<i>Nummulites</i> , many <i>Assilina</i> , SBF, PF, mollusks, echinoids, worms tubes
		21.00	Biocalcarenite	Nummulitids, gastropods, bivalves, corals	<i>Nummulites</i> , orthofragmines, SBF, PF, mollusks, echinoids, worms tubes
		14.50	Biocalcarenite	Gastropods, bivalves	<i>Nummulites</i> , orthofragmines, <i>Assilina</i> , SBF, mollusks, worms tubes
T5	23.50	3.50	Calcarenite	Not recorded	<i>Nummulites</i> , orthofragmines, SBF, PF, mollusks, echinoids, worms tubes
		20.00	Calcarenite	Not recorded	<i>Nummulites</i> , PF, mollusks
T4	18.50	5.00	Biocalcarenite	Many gastropods, many oysters, bivalves, corals	<i>Nummulites</i> , orthofragmines, <i>Assilina</i> , SBF, PF, mollusks
		1.00	Biocalcilitite	Many gastropods, bivalves, corals	PF
		6.00	Biocalcarenite	Many gastropods, many oysters, bivalves, corals	<i>Nummulites</i> , orthofragmines, <i>Assilina</i> , SBF, PF, mollusks
		6.00	Biocalcilitite	Many gastropods, progressive increase in oysters abundance, many bivalves, corals	<i>Nummulites</i> , orthofragmines, <i>Assilina</i> , SBF, mollusks, echinoids
T3	8.00	0.50	Marl	Not recorded	N.a
		8.00	Biocalcilitite	Very rare nummulitids, many gastropods, bivalves, corals	<i>Nummulites</i> , <i>Assilina</i> , SBF, PF, mollusks, corals

Table 1 (continued)

Olivetta section					
Interval	Total Thickness (m)	Layer Thickness (m)	Lithology	Fossil content	
				Outcrop	Thin Section
T2	31.50	1.25	Biocalcissiltite	Progressive reduction of nummulitids abundance	<i>Assilina</i> , PF
		1.25	Biocalcissiltite	Progressive reduction of nummulitids abundance	<i>Nummulites</i> , orthophragmines, <i>Assilina</i> , SBF, mollusks, worms tubes
		15.50	Biocalcirudite	Many nummulitids, corals	Many <i>Nummulites</i> , orthophragmines, <i>Assilina</i> , SBF, corals, echinoids
		2.50	Biocalcarenite	Many nummulitids	<i>Nummulites</i> , echinoids
		0.50	Biocalcissiltite	Many nummulitids	<i>Nummulites</i> , mollusks
		0.50	Marl	Not recorded	N.a
		0.50	Biocalcissiltite	Many nummulitids	N.a
		0.50	Marl	Not recorded	N.a
		0.50	Biocalcissiltite	Many nummulitids	N.a
		6.50	Biocalcissiltite	Many nummulitids	N.a
T1	29.50	2.00	Biocalcissiltite	Reduction of nummulitids abundance	Many <i>Nummulites</i> , orthophragmines, <i>Assilina</i>
		5.00	Biocalcirudite	Many nummulitids, progressive reduction of gastropods and bivalves abundance, corals	Many <i>Nummulites</i> , orthophragmines, SBF, PF, mollusks, echinoids
		0.25	Marl	Not recorded	N.a
		3.50	Biocalcissiltite	Many nummulitids, gastropods, bivalves, corals	Many <i>Nummulites</i> , orthophragmines, <i>Assilina</i> , SBF, PF, mollusks, echinoids
		6.25	Biocalcarenite	Nummulitids, gastropods, bivalves, corals	Many <i>Nummulites</i> , orthophragmines, <i>Assilina</i> , worms tubes
		1.50	Calcsiltite	Not recorded	Not recorded
		4.50	Biocalcissiltite	Progressive reduction of nummulitids abundance, gastropods, bivalves, corals	Many <i>Nummulites</i> , orthophragmines, <i>Assilina</i> , mollusks, worms tubes, SBF
		7.50	Biocalcarenite	Variations of nummulitids abundance, gastropods, bivalves, corals	Many <i>Nummulites</i> , orthophragmines, mollusks
		1.00	Calcsiltite	Not recorded	Not recorded

Microfacies analysis (thin sections)

Two main clusters are recognized (interpreted as microfacies mA and mB), subdivided into eight subfacies (Figs. 2a, b, 4b, 5; Table 1; Supplementary Table S1).

Microfacies mA1 (Fig. 5a): mudstone with scarce biogenic content (<10%) composed of *Nummulites*, *Assilina*, smaller benthic foraminifera (SBF), and planktonic foraminifera. Most of the samples referred to this microfacies are recorded at the top of the section. The siliciclastic content consists of well-sorted but rare quartz grains.

Microfacies mA2 (Fig. 5b): mudstone with scarce biogenic content, such as *Nummulites* and mollusks, with no additional taxa. The siliciclastic content is marked by very fine-to-fine, well-sorted quartz grains.

Microfacies mA3 (Fig. 5c): bioclastic wackestone containing *Nummulites* and mollusks, and very rare *Assilina*,

orthophragmines, planktonic foraminifera, and echinoids. It contains siliciclastic components as well-sorted quartz grains, except in sample Ol-38J.

Microfacies mB1 (Fig. 5d): bioclastic wackestone characterized by a high diversity of fauna, especially larger (*Nummulites* and *Assilina*) and smaller foraminifera. A siliciclastic component of moderately to well-sorted quartzose fraction is observed.

Microfacies mB2 (Fig. 5e): bioclastic wackestone with unsorted bioclasts. A siliciclastic fraction, such as unsorted quartz grains, is also present. This microfacies is characterized by the occurrence of orthophragmines and the absence of *Assilina*, in contrast with microfacies mB1.

Microfacies mB3 (Fig. 5f): bioclastic wackestone characterized by unsorted grains and diverse fauna such as *Nummulites* and *Assilina*. Fine to medium, well-sorted quartz grains constitute the siliciclastic fraction.

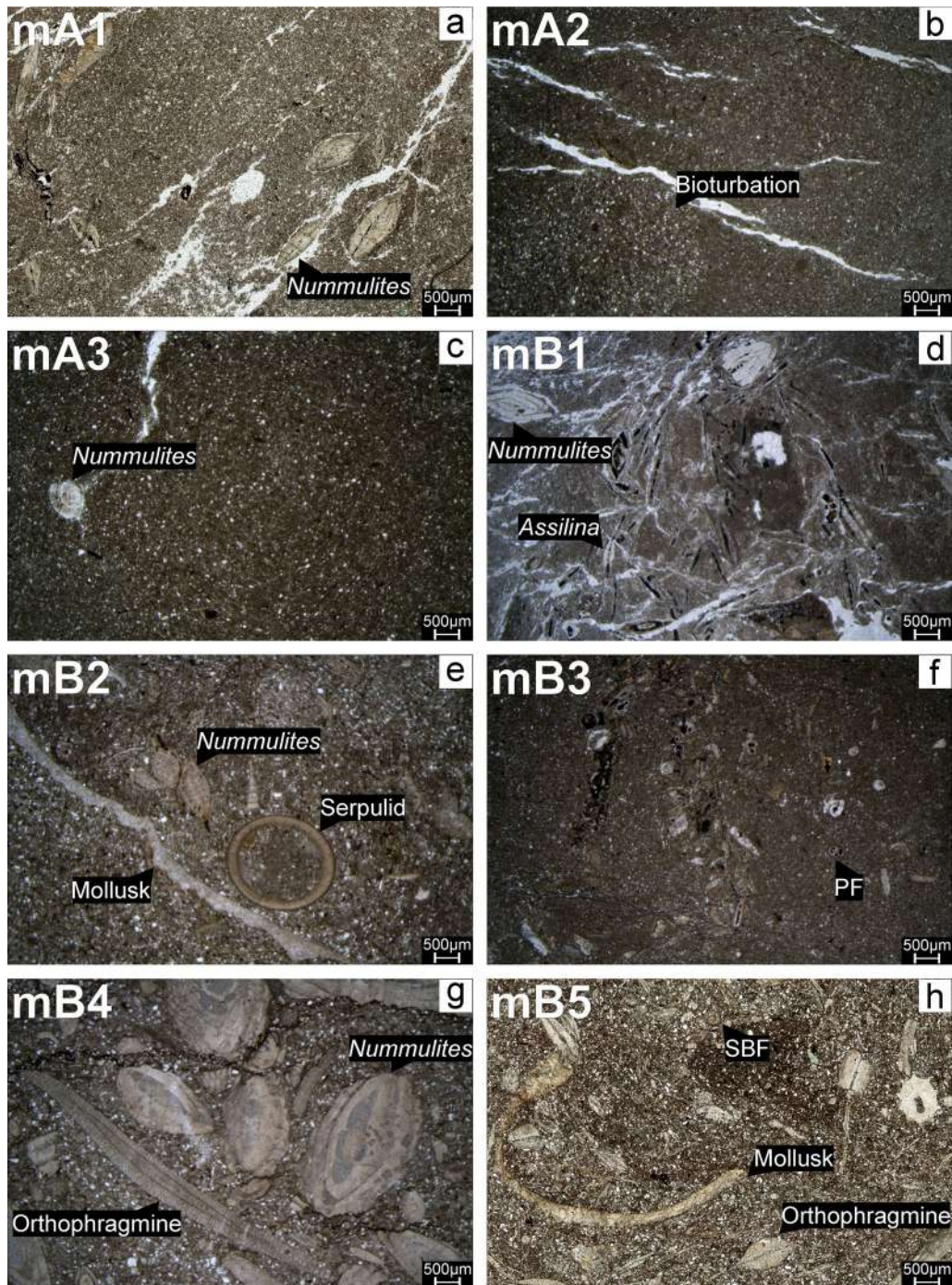


Fig. 5 Photos of the Bartonian microfacies recorded in the Olivetta San Michele section. **a** microfacies mA1 (sample OL-66); mudstone with *Nummulites*. **b** microfacies mA2 (sample OL-47); mudstone with bioturbation. **c** microfacies mA3 (sample OL-46); wackestone with *Nummulites*. **d** microfacies mB1 (sample OL-58); wackestone with *Nummulites* and *Assilina*. **e** microfacies mB2 (sample OL-48);

wackestone with *Nummulites*, mollusks and serpulids. **f** microfacies mB3 (sample OL-57); wackestone with planktonic foraminifera (PF). **g** microfacies mB4 (sample OL-30); packstone with *Nummulites* and orthophragmines. **h** microfacies mB5 (sample OL-73); packstone with mollusks, orthophragmines, and small benthic foraminifera (SBF)

Microfacies mB4 (Fig. 5g): moderately sorted bioclastic packstone rich in biogenic components (mainly orthofragmines and *Nummulites*). Within the siliciclastic component, there are well-sorted quartz grains.

Microfacies mB5 (Fig. 5h): bioclastic packstone characterized by *Nummulites*, *Assilina*, orthofragmines, and small benthic and planktonic foraminifera, except in sample OL-52. This packstone also contains unsorted, rounded to sub-angular bioclasts and fine to medium quartz grains.

Ichnofossil analysis

The samples of the Olivetta SM section have been attributed to 5 ichnofabric (IF) classes, which were named according to the dominant feature and traces. This section describes the major characteristics of each IF class, placing particular emphasis on the degree of bioturbation, the components of the ichnofabric, and the representative intervals of occurrence that are attributable to a specific IF class. When possible, ichnotaxa have been identified at the ichnogenus or ichnospecies level, while open nomenclature is used when precise identification is not possible (Fig. 6).

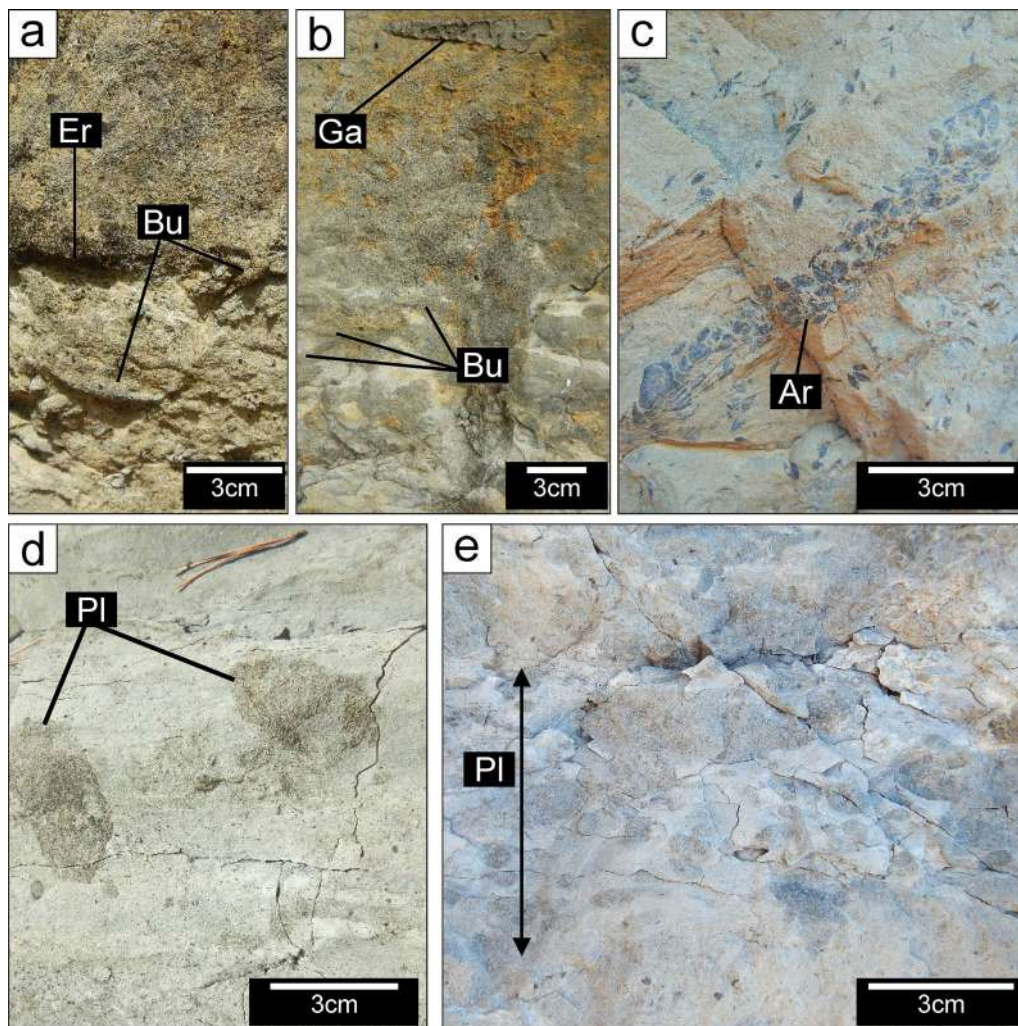


Fig. 6 Ichnofabrics of the Olivetta San Michele section. **a** ‘Coarse-fill burrows’ IF displaying erosive surface (Er) and passively filled burrows (Bu). **b** ‘Coarse-fill burrows’ IF showing numerous passively filled burrows (Bu) and a gastropod (Ga) in a hydrodynamically stable position. **c** ‘*Nummipera*’ IF with a large, armored burrow (Ar).

d ‘*Planolites*’ IF consisting of a *Planolites*-rich horizon (Pl) sandwiched between more homogeneous horizons. **e** Detail of the ‘*Planolites*’ IF showing large specimens of *Planolites*. The interval with the *Planolites* IF (Pl) overlies an interval with the structureless A IF

'Coarse-fill burrows' IF

This ichnofabric occurs in two lithologies, biocalcirudite (from 85 to 95 m) and biocalcisiltite (from 111.50 to 115 m), respectively. It is visually dominated by vertical and oblique burrows that are unlined and filled with sediment. The ichnofabric-forming burrows project from the erosive base of the calcarenite layers into the underlying marl layers (Fig. 6a), where they crosscut the actively filled layers of the *Planolites* IF. The ichnofabric is often associated with gastropods in a hydrodynamically stable position (Fig. 6b). The bioturbation intensity ranges from low (percent bioturbated area: 5–10%) to high (up to 80%) (Supplementary Table S1). The burrows are I, J, and U shaped, but the predominantly vertical exposures prevent a more detailed ichnotaxonomic attribution. These 'coarse-fill burrows' are usually preserved as hyporeliefs at the base of biocalcirudite and biocalcisiltite layers.

Nummipera IF

The ichnofabric is characterized by sparse specimens of *Nummipera eocenica* superimposed on a thoroughly bioturbated background (percent bioturbated area > 80%). The *Nummipera* IF is associated with biocalcarenites and biocalcisiltites with abundant *Nummulites*, which compose the wall of *Nummipera* and associated oblique burrows (Fig. 6c). Bioturbation intensity is homogeneously distributed at the sample scale.

Planolites IF

The ichnofabric consists of horizontal unlined burrows presenting an infill that is darker than the surrounding matrix (*Planolites beverleyensis*; Fig. 6d). The intensity of bioturbation ranges from low (percent bioturbated area < 20%) to high (percent bioturbated area > 80%) (Supplementary Table S1). At the sample scale, bioturbation intensity is homogeneously distributed, but at finer scales of observation, it is frequently (but not exclusively) heterogeneous. Specifically, centimetric horizons with numerous *Planolites* alternate with horizons with few distinct traces (Fig. 6e), showing a regularly heterogeneous distribution of bioturbation. More rarely (e.g., interval 60–65 m), *Planolites*-rich layers alternate with laminated horizons.

Structureless A IF

Structureless A IF is recorded in diverse lithologies (biocalcarenite, biocalcisiltite, and marl) without distinct physical or biogenic structures. Isolated *Planolites* and rare backfilled burrows (*Taenidium*) are documented (e.g., in the interval between 175 and 180 m). Upward transitions

from the structureless A IF to the *Planolites* IF are commonly observed in the stratigraphic intervals 175–185 m and 210–215 m. The transition is gradual and does not involve abrupt lithofacies changes (Fig. 6e).

Structureless B IF

Massive biocalcisiltite, biocalcarenite, and biocalcirudite are rich in gastropods (Fig. 3d) and fragmented bivalves (Fig. 3e). Faint traction laminae and erosive surfaces are occasionally documented. Distinct trace fossils are very rarely observed and consist of vertical J-shaped burrows and *Planolites*-like traces. The outcrop conditions preclude more precise ichnotaxonomic analysis.

Discussion

Paleoecological implications

The Olivetta SM fossil assemblages add an important paleoecological and paleoenvironmental component to our knowledge of this succession. As suggested by the distribution of the fossils and the sedimentology in the sampled section, the assemblages contain typical elements of shallow-water depositional systems (Figs. 2a, b; 6). The biota recorded in the Olivetta SM section, both micro- and macrofauna (larger and smaller foraminifera, mollusks, corals, echinoids, and calcareous worm tubes), are characterized by different life strategies and trophic regimes that are indicative of specific habitats.

The symbiont-bearing larger benthic foraminifera (LBF) play an important role in interpreting the depositional environments as they are, in several horizons of the investigated successions, extremely abundant at both the outcrop and thin section scales, dominating the foraminiferal assemblages. Large, flat, thin-shelled LBF are best adapted in an oligotrophic, low-energy environment and can thrive with very low irradiation (Hottinger 1983; Hallock and Glenn 1986; Eder et al. 2016, 2017, 2018); inflated and giant LBF tests are instead interpreted as adapted to shallower habitats with higher hydrodynamic energy, much closer to the coastline, and with irradiation possibly oscillating due to unstable trophic conditions (Hallock and Glenn 1986; Seddighi et al. 2015; Briguglio et al. 2017; Goeting et al. 2018).

Among the entire LBF community observed, the most abundant are the species belonging to the genus *Nummulites*, which seem to be relatively diverse and extremely abundant in some levels of the succession. The most common species is *N. perforatus*, followed by *N. striatus*, *N. puschi*, and *N. beaumonti*. These taxa are either very large

and inflated (the *N. perforatus* group) or thin and flat (*N. puschi*). Their presence is therefore a clear indication of the shallow-water character of the depositional environment, with oscillating trophic conditions at the seafloor that did not always permit the establishment of a strictly oligotrophic fauna.

Mollusks are recorded both on outcrop surfaces and in thin sections with two taxa: gastropods (Turritellidae) and bivalves (Cardiidae, Ostreidae). Turritellidae thrive both in shallow and deep waters (0–1500 m) under normal marine salinity; nevertheless, some species are able to inhabit brackish and estuarine environments (Allmon 1988; Martinius 1995). They are infaunal, semi-infaunal, or epifaunal suspension feeders and herbivores (Allmon 1988). Turritellids are common throughout the section and occur in different sizes; sporadically, they seem to be deposited with imbricated geometries indicating entrainment on the seafloor. Specimens of the family Cardiidae are also common in the Olivetta SM section: they inhabit preferably muddy and sandy bottoms and burrow just below the surface (shallow infaunal conditions), thriving in shallow to deep waters (Cossignani and Ardevini 2011; Moussavou 2015). The occurrence of Cardiidae in deeper water is dependent on light penetration because they are substrate sensitive and photosensitive and can only inhabit clear water (Martinius 1995). The trophic strategy is associated with suspension-feeding organisms for which organic matter in suspension is available (Moussavou 2015).

Ostreids only occur at specific horizons (111.50–129.50 m; Fig. 2a) and appear suddenly and abundantly; their size ranges between 10 and 20 cm. They are all laying horizontally on the bed surface, none seems to be vertically stacked among others, and they do not show signs of transport (Fig. 3g, h). Oysters inhabit coastal, shallow-, and deep-shelf marine environments in salty or brackish coastal waters. They have the capacity to adapt both to hard and soft substrates and are filter feeders (Machalski 1998; Toscano et al. 2018).

Scleractinian corals are recorded in low abundance in almost the entire section. They thrive mainly in shallow waters, and solitary scleractinian corals can partially withstand turbidity and enhanced sedimentation under constant terrigenous input (Sanders and Baron-Szabo 2005).

Serpulids and echinoids are rare in the studied section, the former being only recorded in thin sections. Calcareous worm tubes belong to serpulids (*Ditrupa*) inhabiting soft sediments on the continental shelf, and their mode of feeding may vary from filter to deposit feeders (Sanfilippo 1999; Hartley 2014). Serpulids are rare in the first meters of the Olivetta SM section, but they become more common in the upper part of the succession. Echinoids inhabit shallow water as epibenthic grazers (herbivores), preferably on sandy or limy bottoms (Mancosu and Nebelsick 2020). The

presence of echinoids is sporadic and scarce in the Olivetta SM section. The spines recorded in thin sections might indicate that they belong to regular echinoids.

Paleoenvironmental reconstruction of the Olivetta SM section

Based on the data retrieved from macrofacies, microfacies, the paleoecological constraints of all retrieved taxa, and all ichnofabrics identified, a subdivision of the stratigraphic section into seven paleoenvironmental intervals is proposed (T1–T7; Figs. 2a, b; 7, 8).

The abundance of nummulitids increases from T1 to T2, and it is here interpreted as the emerging dominance of a very well-suited taxon in a depositional environment that fits its physiological needs: i.e., within the photic zone and with gently agitated waters. Nummulitids are photosymbiont-bearing protists that need to live on an irradiated seafloor to permit photosynthetic activity in their symbionts (e.g., Hottinger 1983; Hohenegger et al. 2019). They may dominate relatively quickly over the other autotrophic taxa, and this is evident between intervals T1 and T2. The demise of suspension-feeder mollusks (turritellids and cardiids) is here interpreted as the consequence of the ecological dominance of nummulitids that tend to saturate substrate availability, rather than invoking a possible reduction of suspended material supply. Ecological conditions seem to point to normal marine salinity conditions and a possible water depth limited to the first 30 m in the absence of high hydrodynamic energy. The presence of *Nummipera eocenica* in the intervals T1 and T2 plausibly corresponds to the onset of a deepening trend because this ichnotaxon is frequently associated with early transgressive conditions (Jach et al. 2012; Mendoza-Rodríguez et al. 2020).

During interval T3, nummulitic tests become rarer and display a strong size reduction; in contrast, corals and mollusks, which are very rare to absent in T2, appear again and occur in relatively high numbers. This variation is due to an increase in sedimentation and water turbidity that might have favored suspension feeders and grazers (gastropods) against autotrophic organisms. The estimated water depth is about 30–40 m, a depth that, in case of enhanced turbidity, easily wipes out most of the LBF communities (Beavington-Penney et al. 2006; Tomassetti et al. 2016; Coletti et al. 2021).

During the interval T4, mollusks become dominant, and an increasing dominance of oysters is seen at outcrop scale. A possible explanation for such a sudden abundance could be associated with increased nutrient input and reduced salinity due to enhanced continental runoff. This is corroborated by the shift in the granulometry from fine to medium (wackestone). Similar events of oyster mass occurrences are described for the Cretaceous

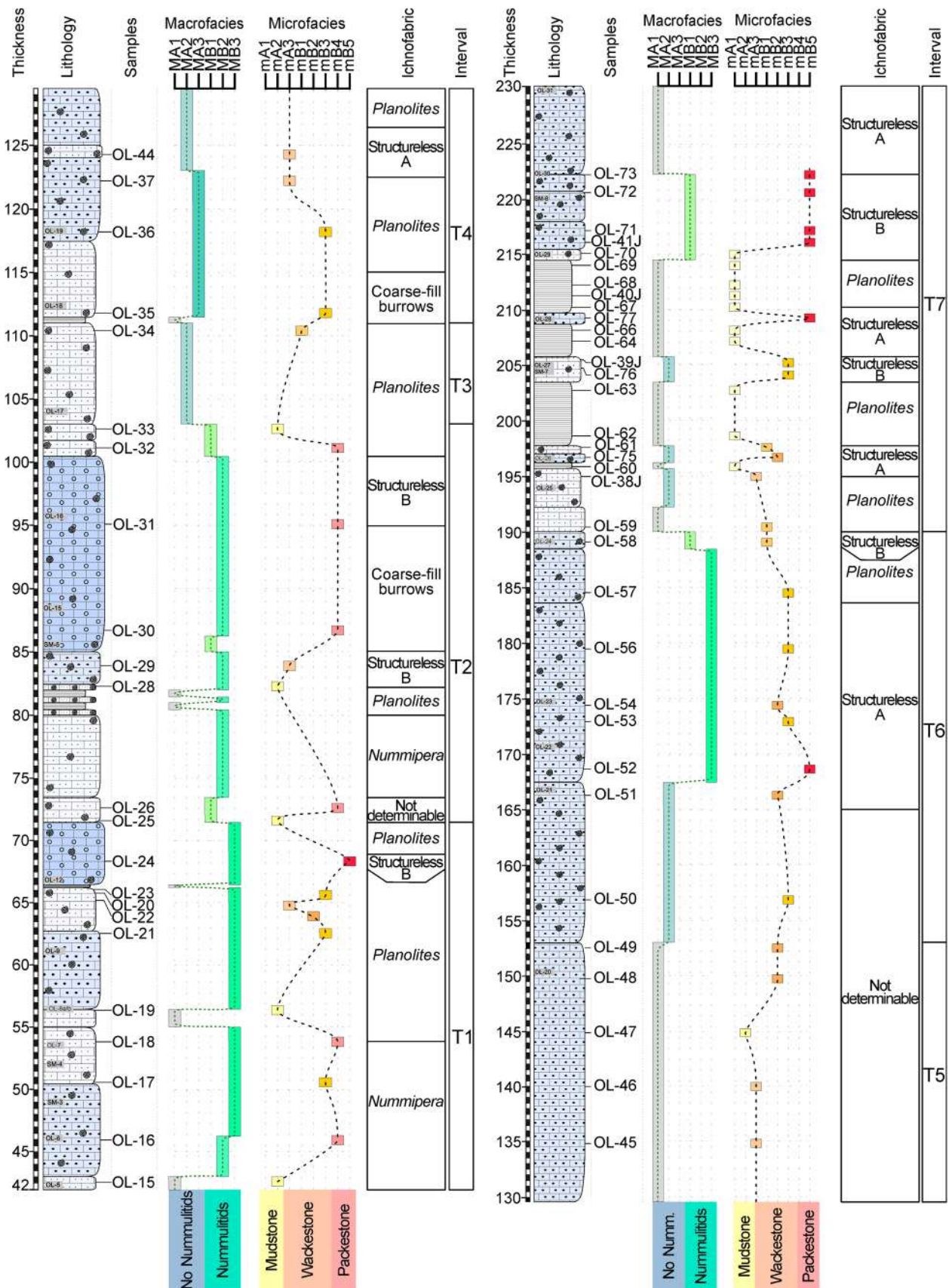
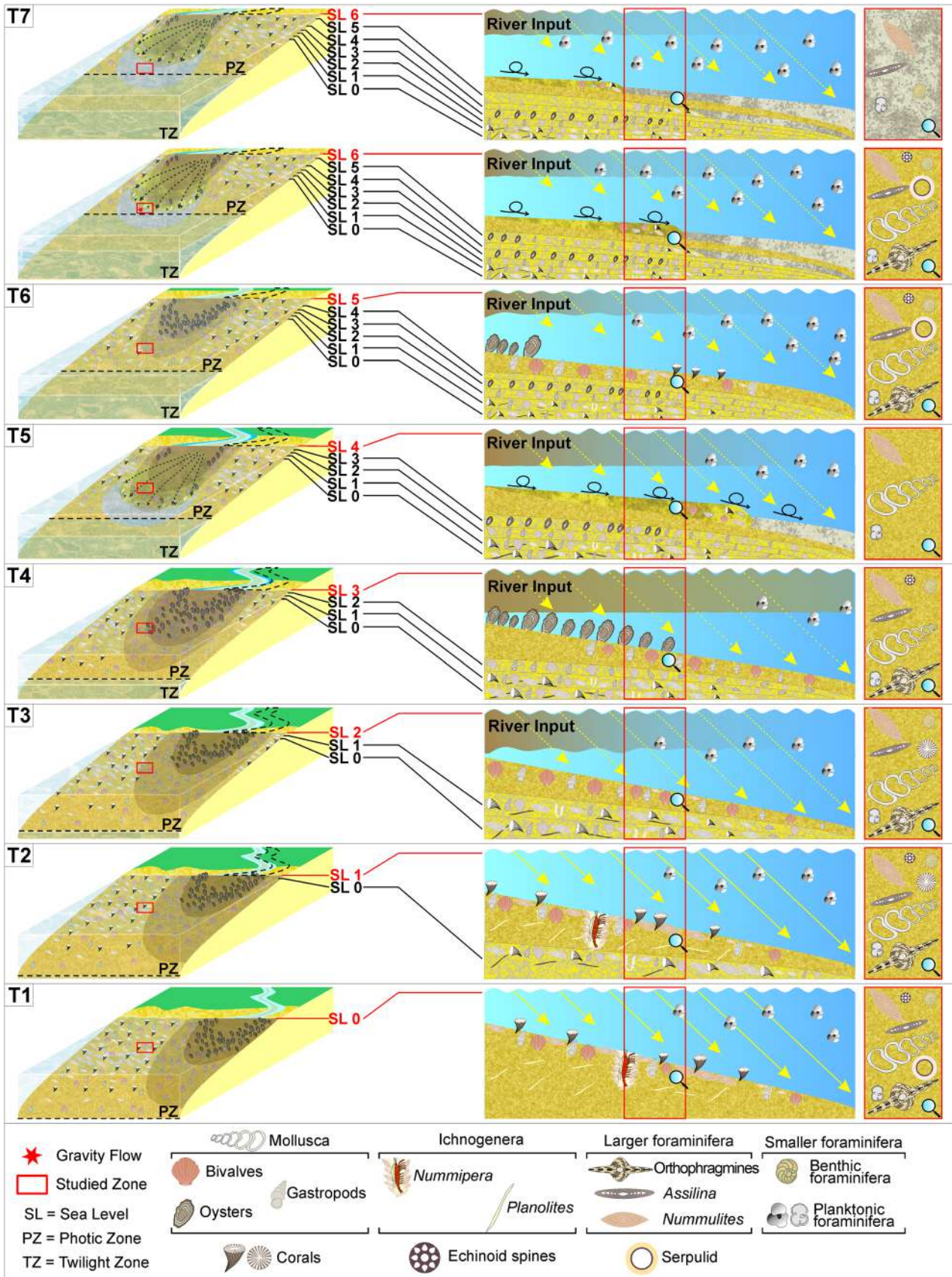


Fig. 7 Correlation of the micro- and macrofacies displaying the ichnofabric characteristics in each paleoenvironmental interval



◀**Fig. 8** Paleoenvironmental evolution of the carbonate ramp at the Olivetta San Michele section, showing the benthic and planktonic communities in the different intervals of time (from T1 to T7) during the Bartonian

of west-central Argentina (Toscano et al. 2018). The ichnofabrics in this interval represent a pre-depositional suite of trace fossils, i.e., the burrows formed prior to event deposition (Uchman and Wetzel 2012). The top of this interval is characterized by *Planolites* IF, which reflects increasing sedimentation rates and commonly indicates fluctuations in oxygen and nutrient contents. The inferred water depth of T4 might still fit at a similar level as previously proposed (interval T4; Figs. 7, 8).

The interval T5 is characterized by the sudden disappearance of all body and trace fossils; the only occurrences seen in the thin sections consist of rare small LBF tests and mollusk fragments. This nearly barren condition is difficult to explain, as organisms should be thriving both on and beneath the seafloor in shallow-water settings. Enhanced sedimentation as well as hypoxic conditions in bottom waters should not be considered because such intervals enhance the preservation of pelagic and planktonic fauna that settles to the seafloor in the absence of scavengers and bioturbators (e.g., Savrda and Bottjer 1991; Wilby et al. 2004; Smith and McGowan 2008). Thus, a possible explanation could be linked to intense hydrodynamic conditions at the seafloor with still enhanced turbidity in the top layers of the water column; this might strongly affect the benthic community, removing all eventually available taxa from that portion of the seafloor. We assume that the river's frontal position favored an increased supply of terrigenous material, displacing all taxa out of the area and causing a barren scenario (interval T5; Figs. 7, 8). Possible variation in salinity produced by riverine supply may be considered a stressful factor for the biota, as recorded in this interval (e.g., Tomanek 2014).

This scenario changes completely in interval T6, where both micro- and macrofauna (diverse LBF taxa, gastropods, corals, SBF, and PF) are recorded again in the sedimentary succession. LBF tests are commonly dispersed in the matrix, but sporadically they are accumulated in irregular patterns, as is typical for the effects of sediment bioturbation. In a few cases, iso-oriented tests may indicate a mild seafloor current and the traction carpet effect (Racey 2001; Gingras et al. 2011, 2015; Kövecsi et al. 2022). Such evidence fits with an active deltaic system where hyperpycnal flows may have similar impacts on seafloors rich in nummulitic tests or may be the consequence of subtidal currents that have similar effects (interval T6; Figs. 7, 8). The sea floor must have been again favorable for a new development of the fauna, but the water depth must have become much deeper within the photic zone,

which in this scenario could have been placed at 50 to 60 m of water depth, as evidenced by the presence of thin and flat *Assilina* without other LBF (Hottinger 1983; Coletti et al. 2021).

The interval T7 is characterized by an alternation of calcisiltite, biocalcisiltite, calcarenite, and biocalcarenite beds with several marly horizons. Biocalcisiltite and biocalcarenite beds have erosive basal contacts and are rich in LBF tests, mostly broken or abraded, thus making them almost nummulithoclastic deposits, here interpreted as high-energy transportation events. These events displaced LBF tests, coming from the more proximal portion of the ramp, into a much deeper setting (interval T7; Figs. 7, 8). The marly sediments are rich in pelagic and planktonic organisms and are therefore interpreted as background sedimentation in deeper and calmer depositional settings.

Trace fossils that are produced very close to the sediment surface tend to be preserved only when they are partly scoured and cast (Uchman and Wetzel 2012); therefore, the absence of the 'coarse-fill burrows' IF suggests that gravity flows were weaker and therefore more distal. Consequently, they might have had not enough energy to preserve shallow-tier burrows, thus confirming the deepening trend suggested by body fossils and sedimentological features (Ferrando et al. 2021) (interval T7; Figs. 7, 8).

The presence of repeated gravity flows may have been favored by global climatic and environmental variations that are well known through the MECO (Zachos et al. 2001): in fact, the sudden increase in temperature could have enhanced precipitations and the hydrological cycle with consequences on the terrigenous flow, as seen already in different basins of the NW Tethys (Held and Soden 2006; Chou et al. 2013; Marvel and Bonfils 2013; Baatsen et al. 2020). This climate variation is known to have caused an alternation between arid and humid conditions, which seems typical of the MECO (e.g., Turkey: Rego et al. 2018; Spain: Peris Cabré et al. 2023; Tunisia: Messaoud et al. 2023; Italy: Gandolfi et al. 2023; Briguglio et al. 2024). In shallow-marine settings, the prolonged warming of the atmosphere and ocean system triggered sediment production despite the underlying transgressive phase, thus registering variations in terrigenous supply along the Provençal Domain (Giammarino et al. 2009; Dallagiovanna et al. 2012a, b). The MECO event coincides with the drowning of the Eocene ramp, which is a regional event in NW Tethys that correlates with the Franco-Italian Maritime Alps and eastern Switzerland sections (Sayer 1995; Sinclair et al. 1998; Allen et al. 2001; Varrone and Clari 2003; Gandolfi et al. 2023). The rapid subsidence of the basin is not only the most important factor that favored the regional drowning ramp, but also the increase in nutrient supply might reduce the productivity of the carbonate ramp because of the renewal of terrigenous input into the distal part of the basin (Hallock and Schlager 1986; Sayer 1995).

Conclusions

The studied sedimentary succession of Olivetta SM is characteristic of a carbonate ramp that formed during the middle Eocene (Bartonian) in the western Tethys, representing a transgressive phase of the basin in the Provençal Domain.

The lower part of the Olivetta SM section is dominated by photosymbiont-bearing organisms that indicate high irradiation and low turbidity in the water column with minimal disturbance by the deltaic system. Gradually, the increase in the terrigenous input firstly favored the proliferation of the filter feeders, then produced a barren interval. Toward the top of the section, the MECO event is registered and can be recognized as an alternation of gravity flows, with a higher diversity of organisms (including LBF) and silty marls, which are barren of macrofossils but rich in foraminifera, especially planktonic.

The retrieved data have shown with high resolution how environmental changes had a direct impact on the benthic community of the NW Tethys: the constant enhancement of riverine inputs that supplied nutrients increased water turbidity and reduced the penetration of solar radiation. These factors, coupled with the general transgressive trend, led to the complete collapse of the benthic carbonate producers. The MECO event in shallow-water sediments does not imply a significant increase in temperature as it does in deeper settings, but it still had a major impact on the benthic community as it triggered precipitations and thus increased the sedimentation rate.

We recognize that identifying global climatic events in shallow-water deposits seems much harder than in deeper settings; only a combination of different field data may shed light on the event occurrence and its effect on the biota. Microfacies analysis, outcrop scale observation, and ichnofabric distribution have proven to be robust enough to accurately describe the effect of MECO on the biota in a shallow-water depositional scenario. This opens new research goals and perspectives because shallow-water settings are those more affected by the ongoing climatic perturbation, and more data are needed from the fossil record during climatic analogs, especially in the Cenozoic.

Supplementary Information The online version contains supplementary material available at <https://doi.org/10.1007/s10347-023-00677-4>.

Acknowledgements This study was supported by the University of Genova, which funded a Curiosity Driven Project awarded to AB on Ligurian Palaeoenvironments and the FRA 2022 Project of MP, and by the Ministry of Education, University and Research (MIUR), Italy, which awarded to AB, MP, and CAP a PRIN 2017 research project labeled “Biota resilience to global change: biomineralization of planktic and benthic calcifiers in the past, present and future” (prot.2017RX9XXY). The authors thank Wolfgang Eder (formerly at the University of Genova), Sulia Goeting (University of Lausanne), and Eleni Lutaj (University of Genova) for their help in the field. They

would also like to thank Wolfgang Kießling, Editor-in-Chief, and the two anonymous reviewers for their constructive comments and suggestions that improved the quality of the manuscript.

Author contributions LA, VMGG, ABr, ABa, JP, CAP, and MP were responsible for field sampling; LA, VMGG, MP, and ABr processed the samples; LA, VMGG, ABa, ABr, CAP, MP, JP, and AG contributed to interpretation, writing, and review. LA, VMGG, ABa, MP, CAP, JP, and ABr were involved in review and editing.

Funding Open access funding provided by Università degli Studi di Genova within the CRUI-CARE Agreement. This study was supported by the University of Genova, which funded the Curiosity Driven Project awarded to AB on Ligurian Palaeoenvironments, and by the Ministry of Education, University and Research (MIUR), Italy, which funded the PRIN 2017 “Biota resilience to global change: biomineralization of planktic and benthic calcifiers in the past, present and future” (prot.2017RX9XXY). MP thanks FRA 2022 University of Genova for the support of this project.

Data availability The authors declare that the data supporting the findings of this study are available within this paper.

Declarations

Conflict of interest The authors have no competing interests to declare that are relevant to the content of the article and did not receive support from any organization for the submitted work.

Open Access This article is licensed under a Creative Commons Attribution 4.0 International License, which permits use, sharing, adaptation, distribution and reproduction in any medium or format, as long as you give appropriate credit to the original author(s) and the source, provide a link to the Creative Commons licence, and indicate if changes were made. The images or other third party material in this article are included in the article’s Creative Commons licence, unless indicated otherwise in a credit line to the material. If material is not included in the article’s Creative Commons licence and your intended use is not permitted by statutory regulation or exceeds the permitted use, you will need to obtain permission directly from the copyright holder. To view a copy of this licence, visit <http://creativecommons.org/licenses/by/4.0/>.

References

- Allen PA, Burgess PM, Galewsky J, Sinclair HD (2001) Flexural-eustatic numerical model for drowning of the Eocene perialpine carbonate ramp and implications for Alpine geodynamics. *Geol Soc Am Bull* 113(8):1052–1066
- Allmon WD (1988) Ecology of recent turritelline gastropods (Prosobranchia, Turritellidae): Current knowledge and paleontological implications. *Palaios* 3(3):259–284. <https://doi.org/10.2307/3514657>
- Apps G, Peel F, Elliott T (2004) The structural setting and palaeogeographical evolution of the Grès d’Annot basin. *Geol Soc Lond Spec. Pub.* 221(1):65–96. <https://doi.org/10.1144/GSL.SP.2004.221.01.05>
- Baatsen M, von der Heydt AS, Huber M, Kliphuis MA, Bijl PK, Sluijs A, Dijkstra HA (2020) The middle to late Eocene greenhouse climate modelled using the CESM 1.0.5. *Clim past* 16(6):2573–2597. <https://doi.org/10.5194/cp-16-2573-2020>
- Beavington-Penney SJ, Wright VP, Racey A (2006) The middle Eocene Seeb Formation of Oman: an investigation of acyclicity,

- stratigraphic completeness, and accumulation rates in shallow marine carbonate settings. *J Sediment Res* 76(10):1137–1161
- Bijl PK, Schouten S, Sluijs A, Reichert GJ, Zachos JC, Brinkhuis H (2009) Early Palaeogene temperature evolution of the southwest Pacific Ocean. *Nature* 461(7265):776–779. <https://doi.org/10.1038/nature08399>
- Bohaty SM, Zachos JC (2003) Significant Southern Ocean warming event in the late middle Eocene. *Geology* 31(11):1017. <https://doi.org/10.1130/G19800.1>
- Bohaty SM, Zachos JC, Florindo F, Delaney ML (2009) Coupled greenhouse warming and deep-sea acidification in the Middle Eocene. *Paleoceanography*. <https://doi.org/10.1029/2008pa001676>
- Boussac J (1912) Études stratigraphiques sur le Nummulitique alpin. *Mém. Serv. Carte Géol. Fr., Paris*. pp 662
- Boscolo Galazzo F, Thomas E, Luciani V, Giusberti L, Frontalini F, Coccioni R (2016) The planktic foraminifer *Planorotalites* in the Tethyan middle Eocene. *J Micropaleontol* 35:79–89. <https://doi.org/10.1144/jmpaleo2014-030>
- Bosellini FR, Benedetti A, Budd AF, Papazzoni CA (2022) A coral hotspot from a hot past: The EECO and post-EECO rich reef coral fauna from Friuli (Eocene, NE Italy). *Palaeogeogr Palaeoclimatol Palaeoecol* 607:111284. <https://doi.org/10.1016/j.palaeo.2022.111284>
- Brandano M (2019) The role of oceanographic conditions on Cenozoic carbonate platform drowning: Insights from Alpine and Apennine foreland basins. *Terra Nova* 31(2):102–110. <https://doi.org/10.1111/ter.12375>
- Brandano M, Tomassetti L (2022) MECO and Alpine orogenesis: Constraints for facies evolution of the Bartonian nummulitic and *Solenomeris* limestone in the Argentina Valley (Ligurian Alps). *Sedimentology* 69(1):24–46. <https://doi.org/10.1111/sed.12829>
- Briguglio A, Seddighi M, Papazzoni CA, Hohenegger J (2017) Shear versus settling velocity of recent and fossil larger foraminifera: New insights on nummulite banks. *Palaios* 32(5):321–329
- Briguglio A, Giraldo-Gómez VM, Baucon A, Benedetti A, Papazzoni CA, Pignatti J, Wolfgring E, Piazza M (2024) A middle Eocene shallow-water drowning ramp in NW Italy: from shoreface conglomerates to distal marls. *Newslett Stratigr* 57(1):37–63. <https://doi.org/10.1127/nos/2023/0784>
- Bromley RG (1996) Trace fossils: biology, taphonomy and applications. *Geol Mag* 134(3):409–421
- Campredon R (1977) Les formations paléogènes des Alpes Maritimes franco-italiennes. *Mém H Sér Soc Géol Fr* 9:1–199
- Coletti G, Mariani L, Garzanti E, Consani S, Bosio G, Vezzoli G, Hu X, Basso D (2021) Skeletal assemblages and terrigenous input in the Eocene carbonate systems of the Nummulitic Limestone (NW Europe). *Sedim Geol* 425:106005. <https://doi.org/10.1016/j.sedgeo.2021>
- Chou C, Chiang JCH, Lan CW, Chung CH, Liao YC, Lee CJ (2013) Increase in the range between wet and dry season precipitation. *Nat Geosci* 6(4):263–267. <https://doi.org/10.1038/ngeo1744>
- Cossignani T, Ardovini R (2011) Malacologia mediterranea. *Atlante delle conchiglie del Mediterraneo*. L'Informatore Piceno, Ancona
- Crippa G, Baucon A, Felletti F, Raineri G, Scarponi D (2018) A multidisciplinary study of ecosystem evolution through early Pleistocene climate change from the marine Arda River section. *Italy Quaternary Res* 89:533–562. <https://doi.org/10.1017/qua.2018.10>
- Dallagiovanna G, Fanucci F, Pellegrini L, Seno S, Bonini L, Decarlis A, Maino M, Morelli D, Toscani G, con contributi di Breda A, Vercesi PL, Zizioli D, Cobianchi M, Mancin N, Papazzoni CA (2012a) Note illustrative della Carta Geologica Foglio 257 - Dolceacqua e Foglio 270 - Ventimiglia. pp 75. Regione Liguria. https://www.isprambiente.gov.it/Media/carg/note_illustrative/257_270_Dolceacqua_Ventimiglia.pdf. Accessed 19 Dec 2023
- Dallagiovanna G, Fanucci F, Pellegrini L, Seno S, Decarlis A, Maino M, Toscani G (2012b) Carta Geologica alla scala 1: 25000 Foglio 257 “Dolceacqua” e Foglio 270 “Ventimiglia” con note illustrative
- de Graciansky PC, Roberts DG, Tricart P (2010) The Western Alps, from rift to passive margin to orogenic belt: an integrated geoscience overview. Elsevier
- Decarlis A, Maino M, Dallagiovanna G, Lualdi A, Masini E, Seno S, Toscani G (2014) Salt tectonics in the SW Alps (Italy–France): From rifting to the inversion of the European continental margin in a context of oblique convergence. *Tectonophysics* 636:293–314. <https://doi.org/10.1016/j.tecto.2014.09.003>
- Deprez A, Tesseur S, Stassen P, D’haenens S, Steurbaut E, King C, Claeys P, Speijer RP (2015) Early Eocene environmental development in the Northern Peri-Tethys (Aktulagay, Kazakhstan) based on benthic foraminiferal assemblages and stable isotopes (O, C). *Mar Micropaleontol* 115:59–71. <https://doi.org/10.1016/j.marmicro.2014.11.003>
- Dunham RJ (1962) Classification of carbonate rocks according to depositional textures. In: Ham WE (eds) *Classification of Carbonate Rocks*. AAPG, pp 108–121. Tulsa
- Eder W, Briguglio A, Hohenegger J (2016) Growth of *Heterostegina depressa* under natural and laboratory conditions. *Mar Micropaleontol* 122:27–43
- Eder W, Hohenegger J, Briguglio A (2017) Depth-related morphologies of megalospheric tests of *Heterostegina depressa* d’Orbigny: Biostratigraphic and paleobiological implications. *Palaios* 32(1):110–117
- Eder W, Hohenegger J, Briguglio A (2018) Test flattening in the larger foraminifer *Heterostegina depressa*: predicting bathymetry from axial sections. *Paleobiology* 44(1):76–88
- Ekdale AA, Bromley RG (1983) Trace fossils and ichnofabric in the Kjølbj Gaard Marl, Upper Cretaceous, Denmark. *Bull Geol Soc Denmark* 31:107–119
- Ferrando I, Brandolini P, Federici B, Lucarelli A, Sguerso D, Morelli D, Corradi N (2021) Coastal modification in relation to sea storm effects: application of 3D remote sensing survey in Sanremo Marina (Liguria NW Italy). *Water* 13(8):1–19. <https://doi.org/10.3390/w13081040>
- Flügel E (2012) *Microfacies of Carbonate Rocks: Analysis Interpretation*. Springer Science & Business Media, Berlin
- Folk RL (1959) *Practical Petrographic Classification of Limestones*. AAPG Bull 43:1–38
- Ford M, Duchêne S, Gasquet D, Vanderhaeghe O (2006) Two-phases orogenic convergence in the external and internal Alps. *J Geol Soc London* 163:815–826
- Foster WJ, Garvie CL, Weiss AM, Muscente AD, Aberhan M, Counts JW, Martindale RC (2020) Resilience of marine invertebrate communities during the early Cenozoic hyperthermals. *Sci Repts* 10(1):1–11
- Gandolfi A, Giraldo-Gómez VM, Luciani V, Piazza P, Adatte T, Arena L, Bomou B, Fornaciari E, Frijia G, Kocsis L, Briguglio A (2023) The Middle Eocene Climatic Optimum (MECO) impact on the benthic and planktic foraminiferal resilience from a shallow-water sedimentary record. *Riv Ital Paleontol Stratigr* 129(3):629–651
- Gèze B, Nestéroff W (1968) Notice explicative, carte géol. France (1/50 000), feuille Menton-Nice, B.R.G.M. Orléans
- Gèze B, Lanteaume M, Peyre Y, Vernet J, Nestéroff W (1968) Carte géologique de la France au 1: 50.000, Feuille Menton-Nice, XXXVII-42 et 43. B.R.G.M. Orléans
- Giammarino S, Orezza S, Piazza M, Rosti D (2009) Evidence of syn-sedimentary tectonic activity in the “flysch di Ventimiglia” (Ligurian Alps foredeep basin). *Ital J Geosci* 128(2):467–472. <https://doi.org/10.3301/IJG.2009.128.2.467>

- Giammarino S, Fanucci F, Orezzi S, Rosti D, Morelli D, Cobiainchi M, De Stefanis A, Di Stefano A, Finocchiaro F, Fravega P, Piazza M, Vannucci G (2010) Note Illustrative della Carta Geologica d'Italia alla scala 1:50.000 - Foglio "San Remo" n.258–271. ISPRA - Regione Liguria. pp 130. A.T.I. - System-Cart s.r.l. - L.A.C. s.r.l. - S.EL.CA., Firenze
- Gingras MK, MacEachern JA, Dashtgard SE (2011) Process ichnology and the elucidation of physico-chemical stress. *Sediment Geol* 237:115–134. <https://doi.org/10.1016/j.sedgeo.2011.02.006>
- Gingras MK, Pemberton SG, Smith M (2015) Bioturbation: Reworking sediments for better or worse. *Oilfield Review* 26:46–58
- Giraldo-Gómez VM, Beik I, Podlaha OG, Mutterlose J (2017) The micropaleontological record 670 of marine early Eocene oil shales from Jordan. *Palaeogeogr Palaeoclimatol Palaeoecol* 485:723–739. <https://doi.org/10.1016/j.palaeo.2017.07.030>
- Goeting S, Briguglio A, Eder W, Hohenegger J, Roslim A, Kocsis L (2018) Depth distribution of modern larger benthic foraminifera offshore Brunei Darussalam. *Micropaleontol* 64(4):299–316
- Grabau AW (1904) On the classification of sedimentary rocks. *American Geologist* 33:228–247
- Hallock P, Glenn EC (1986) Larger foraminifera: a tool for paleoenvironmental analysis of Cenozoic carbonate depositional facies. *Palaios* 1:55–64
- Hallock P, Schlager W (1986) Nutrient excess and the demise of coral reefs and carbonate platforms. *Palaios* 1:389–398
- Hammer Ø, Harper DA, Ryan PD (2001) PAST: Paleontological statistics software package for education and data analysis. *Palaeontol Electron* 4(1):9
- Hartley JP (2014) A review of the occurrence and ecology of dense populations of *Ditrupa arietina* (Polychaeta: Serpulidae). *Mem Mus Victoria* 71:85–95
- Held IM, Soden BJ (2006) Robust responses of the hydrological cycle to global warming. *J Clim* 19(21):5686–5699. <https://doi.org/10.1175/jcli3990.1>
- Hohenegger J, Kinoshita S, Briguglio A, Eder W, Wöger J (2019) Lunar cycles and rainy seasons drive growth and reproduction in nummulitid foraminifera, important producers of carbonate buildups. *Sci Rep* 9(1):8286
- Hollis CJ, Beu AG, Crampton JS, Crundwell MP, Morgans HEG, Raine JI, Jones CM (2010) Boyes AF (2010) Calibration of the New Zealand Cretaceous-Cenozoic Timescale to GTS2004. *GNS Sci Rep* 43:1–20
- Hollis CJ, Taylor KWR, Handley L, Pancost RD, Huber M, Creech JB, Hines BR, Crouch EM, Morgans HEG, Crampton JS, Gibbs S, Pearson PN, Zachos JC (2012) Early Paleogene temperature history of the Southwest Pacific Ocean: Reconciling proxies and Models. *Earth Planet Sci Lett* 349–350:53–66. <https://doi.org/10.1016/j.epsl.2012.06.024>
- Hottinger L (1983) Processes determining the distribution of larger foraminifera in space and time. *Utrecht Micropaleontol Bull* 30:239–253
- Ivany LC, Lohmann KC, Hasiuk F, Blake DB, Glass A, Aronson RB, Moody RM (2008) Eocene climate record of a high southern latitude continental shelf: Seymour Island. *Antarctica Geol Soc Am Bull* 120(5–6):659–678
- Jach R, Machaniec E, Uchman A (2012) The trace fossil *Nummipera eocenica* from the Tatra Mountains, Poland: Morphology and palaeoenvironmental implications. *Lethaia* 45:342–355. <https://doi.org/10.1111/j.1502-3931.2011.00289.x>
- Knaust D (2017) Atlas of Trace Fossils in Well Core: Appearance, Taxonomy and Interpretation. Springer, Cham
- Knaust D (2021) Ichnofabric. In: *Encyclopedia of geology*, 2nd Edn. Elsevier, pp 520–531. <https://doi.org/10.1016/B978-0-12-409548-9.12051-2>
- Kövecsi SA, Less G, Pleş G, Bindiu-Haitonic R, Briguglio A, Papazoni CA, Silye L (2022) *Nummulites* assemblages, biofabrics and sedimentary structures: The anatomy and depositional model of an extended Eocene (Bartonian) nummulitic accumulation from the Transylvanian Basin (NW Romania). *Palaeogeogr Palaeoclimatol Palaeoecol* 586:110751
- Lanteaume M (1968) Contribution à l'étude géologique des Alpes Maritimes franco-italiennes. *Mém. serv. Carte Géol. France*, 1–405
- Lemoine M, Bas T, Arnaud-Vanneau A, Arnaud H, Dumont T, Gidon M, Bourbon M, de Graciansky PC, Rudkiewicz JL, Megard-Galli J, Tricart P (1986) The continental margin of the Mesozoic Tethys in the western alps. *Mar Petrol Geol* 3(3):179–199. [https://doi.org/10.1016/0264-8172\(86\)90044-9](https://doi.org/10.1016/0264-8172(86)90044-9)
- Luciani V, D'Onofrio R, Dickens GR, Wade BS (2017) Planktic foraminiferal response to early Eocene carbon cycle perturbations in the southeast Atlantic Ocean (ODP Site 1263). *Glob Planet Chang* 158:119–133
- Machalski M (1998) Oyster life positions and shell beds from the Upper Jurassic of Poland. *Acta Palaeontol Pol* 43(4):609–634
- Maino M, Seno S (2016) The thrust zone of the Ligurian Penninic basal contact (Monte Fronté, Ligurian Alps, Italy). *J Maps* 12(sup1):341–351. <https://doi.org/10.1080/17445647.2016.1213669>
- Mancosu A, Nebelsick JH (2020) Tracking biases in the regular echinoid fossil record: The case of *Paracentrotus lividus* in recent and fossil shallow-water, high-energy environments. *Palaeontol Electron* 23(2):1–35
- Marchegiano M, John CM (2022) Disentangling the impact of global and regional climate changes during the middle Eocene in the Hampshire Basin: new insights from carbonate clumped isotopes and ostracod assemblages. *Paleoceanogr Paleoclimatol* 37(2):1–13 (e2021PA004299)
- Marini M, Patacci M, Felletti F, Decarli S, McCaffrey W (2022) The erosionally confined to emergent transition in a slope-derived blocky mass-transport deposit interacting with a turbidite substrate, Ventimiglia Flysch Formation (Grès d'Annot System, north-west Italy). *Sedimentology* 69(4):1675–1704. <https://doi.org/10.1111/sed.12968>
- Martín-Martín M, Guerrero F, Tosquella J, Tramontana M (2021) Middle Eocene carbonate platforms of the westernmost Tethys. *Sedim Geol* 415:1–25
- Martinius AW (1995) Macrofauna associations and formation of shell concentrations in the Early Eocene Roda Formation (southern Pyrenees, Spain). *Scripta Geol* 108:1–39
- Marvel K, Bonfils C (2013) Identifying external influences on global precipitation. *Proc Natl Acad Sci USA* 110(48):19301–19306. <https://doi.org/10.1073/pnas.1314382110>
- McIlroy D (2008) Ichnological analysis: The common ground between ichnofacies workers and ichnofabric analysts. *Palaeogeogr Palaeoclimatol Palaeoecol* 270:332–338. <https://doi.org/10.1016/j.palaeo.2008.07.016>
- Mendoza-Rodríguez G, Buatois LA, Rincón-Martínez D, Mángano MG, Baumgartner-Mora C (2020) The armored burrow *Nummipera eocenica* from the upper Eocene San Jacinto Formation, Colombia: morphology and paleoenvironmental implications. *Ichnos* 27:81–91. <https://doi.org/10.1080/10420940.2019.1612391>
- Messaoud JH, Thibault N, De Vleeschouwer D, Monkenbusch J (2023) Benthic biota (nummulites) response to a hyperthermal event: Eccentricity-modulated precession control on climate during the middle Eocene warming in the Southern Mediterranean. *Palaeogeogr Palaeoclimatol Palaeoecol* 626:111712
- Morelli D, Locatelli M, Corradi N, Cianfarra P, Crispini L, Federico L, Migeon S (2022) Morpho-structural setting of the Ligurian

- Sea: The role of structural heritage and neotectonic inversion. *J Mar Sci Eng* 10(9):1176. <https://doi.org/10.3390/jmse10091176>
- Moussavou BM (2015) Bivalves (Mollusca) from the Coniacian-Santonian Anguille Formation from Cap Esterias, northern Gabon, with notes on paleoecology and paleobiogeography. *Geodiversitas* 37(3):315–324
- Mueller P, Maino M, Seno S (2020) Progressive deformation patterns from an accretionary prism (Helminthoid Flysch, Ligurian Alps, Italy). *Geosciences* 10(1):26. <https://doi.org/10.3390/geosciences10010026>
- Papazzoni CA, Čosović V, Briguglio A, Drobne K (2017) Towards a calibrated larger foraminifera biostratigraphic zonation: celebrating 18 years of the application of shallow benthic zones. *Palaios* 32(1–2):1–5
- Pasquini C, Lualdi A, Vercesi PL (2001) Analisi di un sistema deoposizionale costiero nei dintorni di Ventimiglia (Alpi Marittime italo-francesi). *Atti Tic Sc Terra* 42:23–36
- Peris Cabré S, Valerop L, Spangenberg JE, Vinyoles A, Verité J, Adatte T, Tremblin M, Watkins S, Sharma N, Garcés M, Puigdefàbregas C, Castellort S (2023) Fluvio-deltaic record of increased sediment transport during the middle Eocene Climatic Optimum (MECO) Southern Pyrenees Spain. *Egusphere*. <https://doi.org/10.5194/egusphere-2022-891>
- Perotti E, Bertok C, d'Atri A, Martire L, Piana F, Catanzariti R (2012) A tectonically-induced Eocene sedimentary mélange in the West Ligurian Alps, Italy. *Tectonophysics* 568:200–214. <https://doi.org/10.1016/j.tecto.2011.09.005>
- Racey A (2001) A review of Eocene nummulite accumulations: structure, formation and reservoir potential. *J Petrol Geol* 24(1):79–100
- Rego ES, Jovane L, Hein JR, Sant'Anna LG, Giorgioni M, Rodelli D, Özcan E (2018) Mineralogical evidence for warm and dry climatic conditions in the Neo-Tethys (eastern Turkey) during the Middle Eocene. *Palaeogeogr Palaeoclimatol Palaeoecol* 501:45–57. <https://doi.org/10.1016/j.palaeo.2018.04.007>
- Sayer ZR (1995) The Nummulitique: carbonate deposition in a foreland basin setting; Eocene, French alps. PhD Thesis. Durham University. Durham, UK. 351 p. <http://etheses.dur.ac.uk/6103/>. Accessed 19 Dec 2023
- Sanders D, Baron-Szabo RC (2005) Scleractinian assemblages under sediment input: their characteristics and relation to the nutrient input concept. *Palaeogeogr Palaeoclimatol Palaeoecol* 216(1–2):139–181
- Sanfilippo R (1999) *Ditrupea brevis* n. sp., a new serpulid from the Mediterranean Neogene with comments on the ecology of the genus. *Riv Ital Paleontol Stratigr* 105(3):455–464. <https://doi.org/10.1313/2039-4942/5386>
- Savrda CE, Bottjer DJ (1991) Oxygen-related biofacies in marine strata: an overview and update. *Geol Soc Lond Spec Publ* 58(1):201–219. <https://doi.org/10.1144/GSL.SP.1991.058.01.14>
- Seddighi M, Briguglio A, Hohenegger J, Papazzoni CA (2015) New results on the hydrodynamic behaviour of fossil Nummulites tests from two nummulite banks from the Bartonian and Priabonian of northern Italy. *Boll Soc Paleontol It* 54(2):103–116
- Seno S, Fanucci F, Dallagiovanna G, Maino M, Pellegrini L, Vercesi PL, Morelli D, Savini A, Migeon S, Cobiانchi M, Mancin N, Marini M, Felletti F, Decarlis A, Maino M, Toscani G, Breda A, Zizioli D (2012) Carta Geologica alla scala 1:50000 Foglio 257 “Dolceacqua” e Foglio 270 “Ventimiglia”. https://www.isprambiente.gov.it/Media/carg/257_270_DOLCEACQUA_VENTI_MIGLIA/Foglio.html. Accessed 19 Dec 2023
- Serra-Kiel J, Hottinger L, Caus E, Drobne K, Ferrández C, Jauhari AK, Less Gy, Pavlovec R, Pignatti J, Samsó JM, Schaub H, Sirel E, Strougo A, Tambareau Y, Tosquella J, Zakrevskaya E (1998) Larger foraminiferal biostratigraphy of the Tethyan Paleocene and Eocene. *Bull Soc Géol France* 169(2):281–299
- Sinclair HD (1997) Tectonostratigraphic model for underfilled peripheral foreland basins: An Alpine perspective. *Geol Soc Am Bull* 109(3):324–346. [https://doi.org/10.1130/0016-7606\(1997\)109%3c0324:TMFUPF%3e2.3.CO;2](https://doi.org/10.1130/0016-7606(1997)109%3c0324:TMFUPF%3e2.3.CO;2)
- Sinclair HD, Sayer ZR, Tucker ME (1998) Carbonate sedimentation during early foreland basin subsidence: the Eocene succession of the French Alps. *Geol Soc London Spec Publ* 149(1):205–227
- Sluijs A, Zeebe RE, Bijl PK, Bohaty SM (2013) A middle Eocene carbon cycle conundrum. *Nat Geosci* 6(6):429–434. <https://doi.org/10.1038/ngeo1807>
- Smith AB, McGowan AJ (2008) Temporal patterns of barren intervals in the Phanerozoic. *Paleobiology* 34(1):155–161
- Sturani C (1969) Impronte da disseccamento e “torbiditi” nel Luteziano in facies lagunare (“strati a *Cerithium diaboli*” auct.) delle basse valli Roja e Bevera. *Boll Soc Geol Ital* 88:363–379
- Taylor A, Goldring R, Gowland S (2003) Analysis and application of ichnofabrics. *Earth Sci Rev* 60:227–259. [https://doi.org/10.1016/S0012-8252\(02\)00105-8](https://doi.org/10.1016/S0012-8252(02)00105-8)
- Tomanek L (2014) Proteomics to study adaptations in marine organisms to environmental stress. *J Proteomics* 105:92–106. <https://doi.org/10.1016/j.jprot.2014.04.009>
- Tomassetti L, Benedetti A, Brandano M (2016) Middle Eocene sea-grass facies from Apennine carbonate platforms (Italy). *Sedim Geol* 335:136–149
- Torsvik TH, Cocks LRM (2016) Earth history and palaeogeography. Cambridge University Press, Cambridge, pp 317. <https://doi.org/10.1017/9781316225523>
- Toscano AG, Lazo DG, Luci L (2018) Taphonomy and paleoecology of Lower Cretaceous oyster mass occurrences from west-central Argentina and evolutionary paleoecology of gregariousness in oysters. *Palaios* 33(6):237–255. <https://doi.org/10.2110/palo.2017.096>
- Uchman A, Wetzel A (2012) Deep-sea fans. In: Knaust D, Bromley RG (eds) Trace Fossils as Indicators of Sedimentary Environments. *Developments in Sedimentology* 64:643–671. <https://doi.org/10.1016/B978-0-444-53813-0.00021-6>
- Varrone D (2004) Le prime fasi di evoluzione del bacino di avanfossa alpino: la successione Delfinese cretaceo-eocenica, Alpi Marittime. Tesi di Dottorato, Dip. Scienze della Terra, Università degli Studi di Torino
- Varrone D, Clari P (2003) Évolution stratigraphique et paléoenvironnementale de la Formation à Microcodium et des Calcaires à Nummulites dans les Alpes Maritimes franco-italiennes. *Geobios* 36:775–786. <https://doi.org/10.1016/j.geobios.2003.09.001>
- Ward JH (1963) Hierarchical grouping to optimize an objective function. *J Am Stat Assoc* 58(301):236–244. <https://doi.org/10.1080/01621459.1963.10500845>
- Wetzel A, Uchman A (1998) Deep-sea benthic food content recorded by ichnofabrics; a conceptual model based on observations from Paleogene flysch, Carpathians, Poland. *Palaios* 13:533–546. <https://doi.org/10.2307/3515345>
- Wilby PR, Hudson JD, Clements RG, Hollingworth NTJ (2004) Taphonomy and origin of an accumulate of soft-bodied cephalopods in the Oxford Clay Formation (Jurassic, England). *Palaeontology* 47(5):1159–1180. <https://doi.org/10.1111/j.0031-0239.2004.00405.x>
- Zachos J, Pagani M, Sloan L, Thomas E, Billups K (2001) Trends, rhythms, and aberrations in global climate 65 Ma to present. *Science* 292(5517):686–693. <https://doi.org/10.1126/science.1059412>
- Zachos JC, Dickens GR, Zeebe RE (2008) An early Cenozoic perspective on greenhouse warming and carbon-cycle dynamics. *Nature* 451(7176):279–283. <https://doi.org/10.1038/nature06588>